

Physics of singularities in pressure-impulse theory

R. Krechetnikov

Mathematical and Statistical Sciences, University of Alberta, Edmonton, Alberta T6G 2G1, Canada



(Received 22 August 2017; published 16 May 2018)

The classical solution in the pressure-impulse theory for the inviscid, incompressible, and zero-surface-tension water impact of a flat plate at zero dead-rise angle exhibits both singular-in-time initial fluid acceleration, $\partial \mathbf{v} / \partial t|_{t=0} \sim \delta(t)$, and a near-plate-edge spatial singularity in the velocity distribution, $\mathbf{v} \sim r^{-1/2}$, where r is the distance from the plate edge. The latter velocity divergence also leads to the interface being stretched infinitely right after the impact, which is another nonphysical artifact. From the point of view of matched asymptotic analysis, this classical solution is a singular limit when three physical quantities achieve limiting values: sound speed $c_0 \rightarrow \infty$, fluid kinematic viscosity $\nu \rightarrow 0$, and surface tension $\sigma \rightarrow 0$. This leaves open a question on how to resolve these singularities mathematically by including the neglected physical effects—compressibility, viscosity, and surface tension—first one by one and then culminating in the local compressible viscous solution valid for $t \rightarrow 0$ and $r \rightarrow 0$, demonstrating a nontrivial flow structure that changes with the degree of the bulk compressibility. In the course of this study, by starting with the general physically relevant formulation of compressible viscous flow, we clarify the parameter range(s) of validity of the key analytical solutions including classical ones (inviscid incompressible and compressible, etc.) and understand the solution structure, its intermediate asymptotics nature, characteristics influencing physical processes, and the role of potential and rotational flow components. In particular, it is pointed out that sufficiently close to the plate edge surface tension must be taken into account. Overall, the idea is to highlight the interesting physics behind the singularities in the pressure-impulse theory.

DOI: [10.1103/PhysRevFluids.3.054003](https://doi.org/10.1103/PhysRevFluids.3.054003)

I. INTRODUCTION

While research on water-impact phenomena was originally motivated by landing on sea almost a century ago [1], key aspects of the fundamental classical solutions have not yet been fully resolved. In the present work, we will focus on singularities in the classical incompressible inviscid solution corresponding to the potential flow, cf. Fig. 1, right after the impact of a plate of half-width l on a semi-infinite body of liquid of density ρ with velocity V_0 , which does not change in the course of impact if the plate mass is assumed infinite. As formally argued in the classical texts [2–5], if the question is to predict the fluid velocity distribution right after the impact ($t = +0$) on the fluid initially at rest, then neither nonlinear advection nor viscous terms can balance the dominant time derivative, $\partial \mathbf{v} / \partial t$; rather only the sharp pressure gradients can maintain this sudden change in fluid motion,

$$\frac{\partial \mathbf{v}}{\partial t} = -\frac{1}{\rho} \nabla p, \quad (1)$$

where the contributions due to viscosity ν are neglected because any boundary layer formed by a diffusion of viscous effects would grow as $\sqrt{\nu t}$ and thus at $t = +0$ would be infinitely thin. Then the fluid incompressibility, $\nabla \cdot \mathbf{v} = 0$, implies that the pressure p is a harmonic function, $\Delta p = 0$, and thus the fluid motion is potential right after the impact with $\mathbf{v} = \nabla \phi$, where ϕ is the velocity

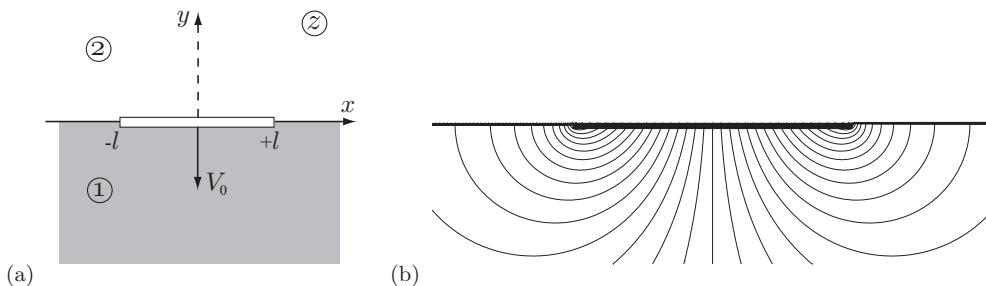


FIG. 1. Plate impact problem: (a) setting, and (b) flow field.

potential, also a harmonic function, $\Delta\phi = 0$. The impulsive nature of the problem is reflected in the fact that the solution of (1) for $t \rightarrow 0$ behaves as $\mathbf{v}(\mathbf{x}, t) \sim H(t)$ and therefore $p(\mathbf{x}, t) \sim \delta(t)$, where $H(t)$ is the Heaviside step function and $\delta(t)$ the Dirac delta function. This is the basis of the classical pressure-impulse theory.

Thus, for $t \rightarrow +0$, one can consider water impact as the boundary value problem in the inviscid potential flow approximation with the boundary conditions at $y = 0$, cf. Fig. 1(a):

$$\text{solid plate, } x \in [-l, l]: \frac{\partial\phi}{\partial y} = -V_0, \quad (2a)$$

$$\text{free interface, } x \notin [-l, l]: \phi = 0, \quad (2b)$$

where the latter condition follows from the fact that the free interface outside the plate footprint is not subject to the pressure impulse and hence the Cauchy-Lagrange integral $\partial\phi/\partial t = -p/\rho$ of (1) after integration from $t = -0$ to $+0$ yields $\phi = 0$ (see also the discussion in Sec. IID). The solution to the above problem was constructed by Lavrentiev and Keldysh [4,6], who recognized that due to the boundary condition for the velocity potential at the free surface, $\phi = 0$, one can extend the flow in a mirror fashion to the upper half-plane so that $\phi(t, x, y) = -\phi(t, x, -y)$ and thus reduce the problem to the motion of a plate in the entire plane using methods of complex analysis. With conformal mapping techniques, the complex potential $f = \phi + i\psi$ relating the velocity potential ϕ and the streamfunction ψ is found to be

$$f(z) = i V_0 (z - \sqrt{z^2 - l^2}), \quad (3)$$

where $z = x + iy$ and the value of $\sqrt{z^2 - l^2}$ is made unique by specifying a branch cut in the z plane along the interval $x \in [-l, l]$; the corresponding streamlines are shown in the laboratory frame of reference in Fig. 1(b). This solution exhibits a singularity at the plate edges in both x and y velocity components $u - iv = f'(z)$ diverging as

$$\mathbf{v} \sim r^{-1/2}, \quad r \rightarrow 0, \quad (4)$$

with r being the radius coordinate positioned at the plate edge. The intuition behind this singular solution is naturally related to the origin of ejecta—in the incompressible case, strictly speaking, the entire fluid body is affected due to the infinite speed of sound propagation, but the volume effectively brought into motion is actually finite, which can be seen from the decay rate of the velocity field: $u - iv \sim (l/z)^2$ for $|z| \rightarrow \infty$. This is, in fact, the explanation as to why the added mass is effectively finite [4] and equal to the half-cylinder of the radius l , cf. Appendix A. Hence, since the mass brought into motion is finite (a half-cylinder under the plate) and the velocity field decays as r^{-2} far from the plate edges, the displaced mass is ejected near the plate edges, where the velocity field is the most singular (4).

If we are interested in the flow near the plate edges, by shifting the coordinate system to, say, the right edge, $z \rightarrow z' + l$, and expanding in z' from (3) we find that

$$(u - iv)e^{-i\theta} = \frac{df}{dz'} = -\frac{ia}{\sqrt{2z'l}} + iV_0 - \frac{3ia}{4\sqrt{2}l^{3/2}}\sqrt{z'} + O(|z'|^{3/2}), \quad (5)$$

where $a = V_0 l$. Thus, the asymptotics (4) is valid for distances close to the edge, $r \ll l$, which is equivalent to the condition that this leading-order term in the velocity components (5) is dominant, i.e., $a/\sqrt{2rl} \gg V_0$. The implication of this observation is that one can justifiably neglect the vertical velocity component of the plate, $-V_0$, i.e., the second term in (5), when analyzing the flow structure near the plate edge, as the key goal is to resolve the singularity in the leading-order pressure-impulse theory. In this (inviscid) approximation, the boundary conditions for the velocity field become homogeneous both at the plate surface (no penetration in the direction \mathbf{n} normal to the plate) and interface:

$$\text{no penetration, } \theta = -\pi: \frac{\partial\phi}{\partial\mathbf{n}} (\equiv v_\theta) = 0, \quad (6a)$$

$$\text{free surface, } \theta = 0: \phi = 0. \quad (6b)$$

In view of the homogeneity of the boundary conditions (6), one may consider the leading-order term in the solution (5) as an *eigensolution* [7] of the Laplace equation with the boundary conditions (6), which gives the leading-order velocity potential [8]:

$$\phi \simeq \sqrt{2l} V_0 r^{1/2} \sin \frac{\theta}{2}. \quad (7)$$

In addition to the singularities at $t \rightarrow 0$ and $r \rightarrow 0$, a singular velocity distribution (4) is nonphysical, as it would lead to an instant infinite stretching of the fluid interface. Since in reality the latter has surface tension, it would mean that after the finite-energy impact the interface attains infinite surface energy, which is impossible since the energy gained by fluid during impact is always finite even if the plate mass is infinite (cf. Appendix A). Thus, surface tension should be present in the leading-order solution [9].

In the present paper, we will elucidate the fundamental aspects of the above singular behaviors. The appropriate problem formulation in the framework of compressible Navier-Stokes equations (NSEs) is given in Sec. II, which is then properly nondimensionalized and scaled. The latter, in particular, allows us to identify the limits of validity of the classical pressure-impulse solution (3), cf. Sec. IID. Next, in the subsequent sections we systematically resolve the spatial and temporal singularities by taking into account viscosity $r \rightarrow 0$ (Sec. III), compressibility $t \rightarrow 0$ (Sec. IV), and finally both viscosity and compressibility $t, r \rightarrow 0$ (Sec. V). In all these sections, we construct solutions analytically, identify their key properties (self-similarity, etc.), the regions of validity in the time-space domain in terms of the key nondimensional parameters (Mach, Reynolds, Weber, etc., numbers), and, where possible, establish the relation between these key solutions, e.g., relaxation of the post shock wave solution to the incompressible one (Sec. IVC). Finally, in the discussion of the early-time viscous compressible solution, we highlight the processes responsible for the resolution of singularities: this is done with the help of mathematical tools—vector field decomposition into irrotational and potential parts (Sec. VA) as well as characteristic analysis (Sec. VB)—and physical insights into the mechanisms responsible for signal propagation, i.e., diffusion and compressible effects. The solution in the viscous compressible region near the plate edge and at early times exhibits a rich structure defined by the dependence on the ratio of the first and second viscosities (Sec. VC). The discussion is concluded in Sec. VI with a summary and some open questions requiring further study.

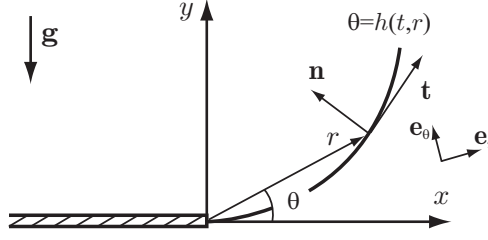


FIG. 2. Near the plate edge region: $\theta = -\pi$ is the plate and $\theta = h(t, r)$ is the liquid interface.

II. PROBLEM FORMULATION AND SCALING

A. Governing equations and boundary conditions

In vector form, the dimensional NSEs governing the plane motion of a compressible fluid of density ρ with velocity \mathbf{v} and pressure p in the gravity field \mathbf{g} are

$$\frac{\partial \rho}{\partial t} + \nabla \cdot (\rho \mathbf{v}) = 0, \quad (8a)$$

$$\rho \left[\frac{\partial \mathbf{v}}{\partial t} + (\mathbf{v} \cdot \nabla) \mathbf{v} \right] = -\nabla p + \nabla \cdot \boldsymbol{\tau} + \rho \mathbf{g}, \quad (8b)$$

where, according to Newton's law of viscosity, the viscous stress tensor $\boldsymbol{\tau}$ reads

$$\boldsymbol{\tau} = \mu [\nabla \mathbf{v} + (\nabla \mathbf{v})^\dagger] + \left(\lambda - \frac{2}{3} \mu \right) (\nabla \cdot \mathbf{v}) \mathbf{I}, \quad (9)$$

with \mathbf{I} being the unit (dyadic) tensor (Kronecker delta function), μ and λ the first and second (bulk) coefficients of viscosity, respectively, both positive [10] for media in thermodynamic equilibrium [11].

The above formulation requires two boundary conditions for each of the velocity components v_r and v_θ , naturally at the plate surface $\theta = -\pi$ and free surface $\theta = h(t, r)$, cf. Fig. 2. At the free surface boundary, one has the dynamic condition—zero net force acting on the interface at a particular point, i.e., the dot product of the vector \mathbf{n} normal to the interface with the total stress tensor $-p \mathbf{I} + \boldsymbol{\tau}$ balanced by the capillary pressure:

$$\theta = h(t, r) : \quad -(-p \mathbf{I} + \boldsymbol{\tau}) \cdot \mathbf{n} = \sigma (\nabla \cdot \mathbf{n}). \quad (10)$$

The interface is also subject to the kinematic condition, which can be written using an implicit representation of the interface, $H = \theta - h(t, r)$:

$$\frac{\partial H}{\partial t} + \mathbf{v} \cdot \nabla H = 0, \quad \text{so that} \quad \frac{\partial h}{\partial t} + v_r \frac{\partial h}{\partial r} = \frac{v_\theta}{r} \quad \text{at} \quad \theta = h(t, r), \quad (11)$$

i.e., the vanishing total (material) derivative—in physical terms, this implies that velocity of the liquid normal to the interface, $\mathbf{n} \cdot \mathbf{v}$ with $\mathbf{n} = \nabla H / |\nabla H|$, should be equal to that of the interface, $H_t / |\nabla H|$, for the sake of the fluid continuity. If the normal and tangential vectors in polar coordinates ($\mathbf{e}_r, \mathbf{e}_\theta$) are defined by

$$\mathbf{n} = \frac{\nabla H}{|\nabla H|} = \frac{-r h_r \mathbf{e}_r + \mathbf{e}_\theta}{\sqrt{1 + r^2 h_r^2}}, \quad \mathbf{t} = \frac{\mathbf{e}_r + r h_r \mathbf{e}_\theta}{\sqrt{1 + r^2 h_r^2}}, \quad (12)$$

then both pairs ($\mathbf{e}_r, \mathbf{e}_\theta$) and (\mathbf{t}, \mathbf{n}) are right-handed coordinate systems. The curvature is

$$\nabla \cdot \mathbf{n}|_{\theta=h(t,r)} = -\frac{1}{r} \frac{1}{(1 + r^2 h_r^2)^{3/2}} [2r h_r + r^2 h_{rr} + r^3 h_r^3], \quad (13)$$

and, in the limit $r \rightarrow 0$, $\nabla \cdot \mathbf{n} \simeq -2h_r - rh_{rr}$ under the appropriate assumptions on the smallness of $r h_r$, which is consistent with the physical requirement [12] that the interface departs from the plate edge $h \rightarrow 0$ as $r \rightarrow 0$.

Finally, we are not going to take into account thermodynamic effects, i.e., we will close the above system with a barotropic fluid equation of state $p = p(\rho)$, which is known to be valid for fluids such as water even at very high pressures [13]. In terms of the deviation p_1 of the pressure from its equilibrium value p_0 , i.e., $p - p_0 = p_1$, the equation of state is given by

$$p_1 = B \left[\left(\frac{\rho}{\rho_0} \right)^n - 1 \right], \quad (14)$$

where $B = \rho_0 c_0^2 / n$ with the following values (for water): $\rho_0 = 1000 \text{ kg/m}^3$, $c_0 = 1500 \text{ m/s}$, and $n = 7.15$. Then the speed of sound for barotropic undisturbed media, i.e., at the density value ρ_0 , is simply

$$c_0 = \sqrt{dp/d\rho|_{\rho_0}}; \quad (15)$$

in particular, the equation of state (14) is consistent with this formula. Also, in the present analysis we are going to assume both viscosities, μ and λ , to be constant.

B. Nondimensionalization

Since we are interested in resolving the physics on the acoustic and longer time scales, the proper time scale is defined by the plate size l and sound speed c_0 . The flow velocity scale is set by the impact velocity V_0 . The pressure scale is estimated based on the loads during the flat-bottomed impact on a compressible liquid surface: as first arrived at by von Karman [1] using Newton's second law [14], the result is on the order of $\rho_0 c_0 V_0$, where c_0 is the sound speed, ρ_0 the density of the liquid, and V_0 the impact velocity. Therefore, using thus motivated nondimensionalization

$$r \rightarrow lr, \quad \mathbf{v} \rightarrow V_0 \mathbf{v}, \quad t \rightarrow \frac{l}{c_0} t, \quad \rho \rightarrow \rho_0 \rho, \quad p \rightarrow \rho_0 c_0 V_0 p, \quad (16)$$

the system (8) reads

$$\frac{\partial \rho}{\partial t} + \text{Ma} \nabla \cdot (\rho \mathbf{v}) = 0, \quad (17a)$$

$$\rho \left[\frac{\partial \mathbf{v}}{\partial t} + \text{Ma} (\mathbf{v} \cdot \nabla) \mathbf{v} \right] = -\nabla p + \frac{\text{Ma}}{\text{Re}} \nabla \cdot \boldsymbol{\tau} + \frac{\text{Ma}}{\text{Fr}^2} \rho \mathbf{e}_g, \quad (17b)$$

with \mathbf{e}_g being the unit vector in the direction of the gravity $\mathbf{g} = g \mathbf{e}_g$ and the nondimensional viscous tensor $\boldsymbol{\tau}$ (9) now given by

$$\boldsymbol{\tau} = [\nabla \mathbf{v} + (\nabla \mathbf{v})^\dagger] + \left(\frac{\lambda}{\mu} - \frac{2}{3} \right) (\nabla \cdot \mathbf{v}) \mathbf{I} = [\nabla \mathbf{v} + (\nabla \mathbf{v})^\dagger] + (\chi - 1) (\nabla \cdot \mathbf{v}) \mathbf{I}, \quad (18)$$

where $\chi = \frac{\lambda}{\mu} + \frac{1}{3}$; the dynamic boundary condition (10) becomes

$$\theta = h(t, r): \quad - \left(-p \mathbf{I} + \frac{\text{Ma}}{\text{Re}} \boldsymbol{\tau} \right) \cdot \mathbf{n} = \frac{\text{Ma}}{\text{We}} (\nabla \cdot \mathbf{n}) \mathbf{n}, \quad (19)$$

and the kinematic (11) furnishes

$$\theta = h(t, r): \quad \frac{1}{\text{Ma}} \frac{\partial h}{\partial t} + v_r \frac{\partial h}{\partial r} = \frac{v_\theta}{r}, \quad (20)$$

where the nondimensional complexes

$$\text{Re} = \frac{\rho_0 V_0 l}{\mu}, \quad \text{Ma} = \frac{V_0}{c_0}, \quad \text{We} = \frac{\rho_0 V_0^2 l}{\sigma}, \quad \text{Fr} = \frac{V_0}{\sqrt{gl}}, \quad (21)$$

are Reynolds, Mach, Weber, and Froude numbers, respectively.

C. Scalings

Next, since we are interested in the early times after the impact event and because of the continuity of the solutions of the fluid dynamics equations, we can consider the regime when density variation can be treated as a perturbation of the initial state ρ_0 ,

$$\rho \rightarrow \rho_0 + \rho, \quad |\rho| \ll \rho_0, \quad (22)$$

i.e., a weakly compressible impact [15]. As a result, propagation of only a weak discontinuity [10]—a compression wave—will be considered here [16]. Hence, if (in dimensional form) the equation of state is $p(\rho)$, then its Taylor series near ρ_0 is

$$p(\rho) = p(\rho_0) + \frac{dp}{d\rho}(\rho_0)(\rho - \rho_0) + \frac{d^2p}{d\rho^2}(\rho_0) \frac{(\rho - \rho_0)^2}{2} + \dots, \quad (23)$$

so that in the nondimensional form we get

$$\frac{p(\rho) - p(\rho_0)}{\rho_0 c_0 V_0} = \frac{c_0^2}{c_0 V_0} \frac{\rho - \rho_0}{\rho_0} + \dots \Rightarrow \delta p = \frac{1}{\text{Ma}} \delta \rho. \quad (24)$$

From the system (17) it is clear that simply putting $\text{Ma} = 0$ or, as motivated by (24), expanding density (and velocity) in a Taylor series $\rho = 1 + \text{Ma}\rho_1 + \text{Ma}^2\rho_2 + \dots$, does not lead to the incompressible NSEs. Hence, as the flow develops in the near-plate-edge region incompressibility can appear (and can be justified) only at certain time and length scales, which are to be determined in Sec. IID.

Let us introduce the following scalings of the already nondimensionalized variables (16):

$$t \rightarrow \kappa^{-1} t, \quad r \rightarrow \epsilon r, \quad \mathbf{v} \rightarrow \delta \mathbf{v}, \quad \rho \rightarrow 1 + \Delta \rho, \quad p \rightarrow \Pi p, \quad (25)$$

where δ need not be small, $\Delta \ll 1$ corresponds to a weakly compressible case, $\kappa = O(1)$ to the compressible flow time scale, and $\kappa \ll 1$ to long-time asymptotics (which is why we use κ^{-1}). Here δ , Δ , and Π in general depend on ϵ , κ , Ma , Re , Fr , and We and are determined as part of the solution. As a result, we get the following scaled continuity equation

$$\Delta \frac{\epsilon}{\delta \text{Ma}} \kappa \frac{\partial \rho}{\partial t} + \Delta[(\mathbf{v} \cdot \nabla)\rho + \rho \nabla \cdot \mathbf{v}] + \nabla \cdot \mathbf{v} = 0, \quad (26)$$

the momentum equation

$$(1 + \Delta \rho) \left[\frac{\partial \mathbf{v}}{\partial t} + \frac{1}{\kappa} \frac{\delta \text{Ma}}{\epsilon} (\mathbf{v} \cdot \nabla) \mathbf{v} \right] = -\frac{\Pi}{\epsilon \delta \kappa} \nabla p + \frac{1}{\kappa \epsilon^2} \frac{\text{Ma}}{\text{Re}} \nabla \cdot \boldsymbol{\tau} + \frac{1}{\delta \kappa} \frac{\text{Ma}}{\text{Fr}^2} (1 + \Delta \rho) \mathbf{e}_g, \quad (27)$$

and the dynamic boundary condition

$$\theta = h(t, r): \quad -\left(-p \mathbf{I} + \frac{1}{\kappa \epsilon^2} \frac{\text{Ma}}{\text{Re}} \boldsymbol{\tau} \right) \cdot \mathbf{n} = \tilde{\sigma} (\nabla \cdot \mathbf{n}) \mathbf{n}, \quad \text{with } \tilde{\sigma} = \frac{1}{\delta \kappa \epsilon^2} \frac{\text{Ma}}{\text{We}}, \quad (28)$$

which in the normal \mathbf{n} and tangential \mathbf{t} components can be written as

$$\theta = h(t, r): \quad \mathbf{n} : p - \frac{1}{\kappa \epsilon^2} \frac{\text{Ma}}{\text{Re}} \mathbf{n} \cdot \boldsymbol{\tau} \cdot \mathbf{n} = \tilde{\sigma} (\nabla \cdot \mathbf{n}), \quad (29a)$$

$$\mathbf{t} : \frac{1}{\kappa \epsilon^2} \frac{\text{Ma}}{\text{Re}} \mathbf{t} \cdot \boldsymbol{\tau} \cdot \mathbf{n} = 0. \quad (29b)$$

Finally, the kinematic boundary condition becomes

$$\theta = h(t, r): \quad \frac{\partial h}{\partial t} = \frac{\delta \text{Ma}}{\epsilon \kappa} \left(-v_r \frac{\partial h}{\partial r} + \frac{v_\theta}{r} \right). \quad (30)$$

In summary, the *a priori* asymptotic assumptions are dictated by the physics

$$\Delta \ll 1, \quad \epsilon \ll 1, \quad \text{Ma} \ll 1, \quad \text{Re}^{-1} \ll 1, \quad (31)$$

which accounts for the small density variation, close distance to the plate edge (compared to the plate size), low Mach number, and low viscosity flow, respectively. Here, strictly speaking, Δ is determined as part of the solution; from the equation of state (24), after application of the scalings (25), we find

$$\Delta = \text{Ma} \Pi. \quad (32)$$

Also, we assume no significant effect of gravity (since the involved initial acceleration due to impact dominates that of gravity):

$$\frac{1}{\delta \kappa} \frac{\text{Ma}}{\text{Fr}^2} \ll 1, \quad (33)$$

which is a valid assumption for sufficiently short (physical) times, and take

$$\Pi = \epsilon \delta \kappa \quad (34)$$

as it is the pressure (gradient) which balances the sudden acceleration $\partial \mathbf{v} / \partial t$ as per the discussion in Sec. I. Given the general asymptotic scalings (31)–(34) we may proceed with different limiting situations: it is only δ , which is found as part of the solution as a function of ϵ , κ , Ma, Re, Fr, and We. Finally, we need

$$\left[\frac{\delta \text{Ma}}{\epsilon} \right] \frac{1}{\kappa} \ll 1, \quad (35)$$

so that the nonlinear terms in (27) can be neglected, thus justifying the formal (physical) argument of classical texts [2–5] mentioned in the introduction.

D. Inviscid incompressible sublimit

With the above general setting, nondimensionalization, and scalings, we are now in a position to clarify the conditions under which the classical solution (3) is valid. From the scaled continuity equation (26), it follows that in order to get an incompressible limit

$$\nabla \cdot \mathbf{v} = 0, \quad (36)$$

the conditions $\Delta \ll 1$ [which is given *a priori* (31) due to weakly compressible impact] and $[\epsilon / (\delta \text{Ma})] \kappa \Delta \ll 1$ must be satisfied, which, taking into account (32) and (34), lead to

$$\text{Ma} \Pi \ll 1, \quad \epsilon \kappa \ll 1 \quad \text{or} \quad \Pi \ll \text{Ma}^{-1}, \quad \epsilon \ll \kappa^{-1}, \quad (37)$$

where the latter condition means that we are far behind the shock wave corresponding to $\epsilon \sim \kappa^{-1}$.

From the momentum equation (27), we need

$$\frac{1}{\kappa \epsilon^2} \frac{\text{Ma}}{\text{Re}} \ll 1, \quad (38)$$

in order to discard the viscous contribution, thus producing the momentum equation, with nonlinearity neglected provided (35) is satisfied:

$$\frac{\partial \mathbf{v}}{\partial t} = -\nabla p. \quad (39)$$

Under the condition (38), the dynamic boundary condition (29) reduces to the normal component only:

$$\theta = h(t, r): \quad p = \tilde{\sigma} \nabla \cdot \mathbf{n} \quad \text{with} \quad \tilde{\sigma} = \frac{1}{\delta \kappa \epsilon^2} \frac{\text{Ma}}{\text{We}}. \quad (40)$$

Note that the inviscid momentum equation (39), i.e., when viscous effects are negligible, stays exactly the same in both compressible and incompressible cases, but the continuity equation naturally changes, as we will see in Sec. IV A.

In summary, the inviscid incompressible sublimit corresponds to the system of bulk motion equations (36) and (39), which, as argued in the introduction, can be reduced to the following problem for the velocity potential ϕ :

$$\Delta\phi = 0, \quad (41a)$$

$$\frac{\partial\phi}{\partial t} = -p, \quad (41b)$$

where the latter equation (Cauchy-Lagrange integral [4]) follows from integration of (39). The (asymptotic) solution of (41) with the boundary conditions (6) near the plate edge is, in dimensional variables, Eq. (7). Applying the scalings (16) and (25) to (7) consecutively, we arrive at the scaling for velocity

$$\delta \sim \epsilon^{-1/2}, \quad (42)$$

i.e., the closer to the plate edge (smaller ϵ), the more singular the velocity; physically, the singularity is due to the fluid particles being squished once they approach the near-plate-edge region [8]. The scaling (42) can be predicted *a priori* by observing that the flow near the plate edge corresponds to the flow around the infinitely thin plate [10], i.e. in the sector of angle 2π , as is also obvious from the derivation of (3). With (42) the condition (35) necessary for neglecting the nonlinearity in (27) becomes

$$\epsilon^{3/2}\kappa \gg \text{Ma} \quad \text{or} \quad \epsilon \gg (\text{Ma}/\kappa)^{2/3}, \quad (43)$$

which means that one also requires $\kappa \gg \text{Ma}$, i.e., to be early enough in time (in particular, compared to the flow time scale l/V_0) and to be far enough from the edge. In addition, to be able to neglect the viscous effects, the distance from the edge must obey $\epsilon \gg \epsilon_{\text{vis}} = \sqrt{\text{Ma}/(\text{Re}\kappa)}$ (viscous length scale) as follows from (38). Based on (43), nonlinearity becomes important at the distance $\epsilon \sim (\text{Ma}/\kappa)^{2/3}$ from the plate edge. In the ideal incompressible limit $\text{Ma} \rightarrow 0$, nonlinearity is not important at any distance from the plate edge. Of course, in reality, Ma is finite and set by the physics, while time scale κ on which we consider the problem can be chosen arbitrarily. Also, as follows from the inequality $\Pi \ll \text{Ma}^{-1}$ derived in (37) and scalings (34) and (42),

$$\epsilon \ll \text{Ma}^{-2}\kappa^{-2}, \quad (44)$$

which is always satisfied as long as $\kappa \leq \text{Ma}^{-2}$; the latter condition is not restrictive for our purposes as we consider the low Mach number $\text{Ma} \ll 1$ and long-time $\kappa \ll 1$ (as per Sec. II C) limits.

Altogether, we get the following inequality conditions for the validity of the inviscid incompressible case with negligible nonlinearity:

$$(\text{Ma}/\kappa)^{2/3} \ll \epsilon \ll \kappa^{-1} \ll \text{Ma}^{-1}, \quad (45)$$

illustrated in Fig. 3 in the (ϵ, κ) plane. Clearly, the curves κ^{-1} and $(\text{Ma}/\kappa)^{2/3}$ may intersect at $\kappa \sim \text{Ma}^{-2}$, which makes $\epsilon = \text{Ma}^2$ and corresponds to a very short time and distance from the edge when nonlinearity is important on the shock wave despite the fact that it was assumed to be weak.

Finally, $\tilde{\sigma}$ in (40) can be put in the form

$$\tilde{\sigma} = \frac{\text{Ma}/\kappa}{\epsilon^{3/2}} \frac{1}{\text{We}}, \quad \text{where} \quad \frac{\text{Ma}/\kappa}{\epsilon^{3/2}} \ll 1 \quad \text{due to (43)}, \quad (46)$$

so that if We is finite from (29a) and (30) in the inviscid case, i.e., when (38) is satisfied, we get the following system of dynamic and kinematic conditions at the interface:

$$\theta = h(t, r): \quad \frac{\partial\phi}{\partial t} = -\tilde{\sigma} \nabla \cdot \mathbf{n}, \quad (47a)$$

$$\frac{\partial h}{\partial t} = \tilde{\delta} \left(-v_r \frac{\partial h}{\partial r} + \frac{v_\theta}{r} \right); \quad v_r = \frac{\partial\phi}{\partial r} \quad \text{and} \quad v_\theta = \frac{1}{r} \frac{\partial\phi}{\partial\theta}, \quad (47b)$$

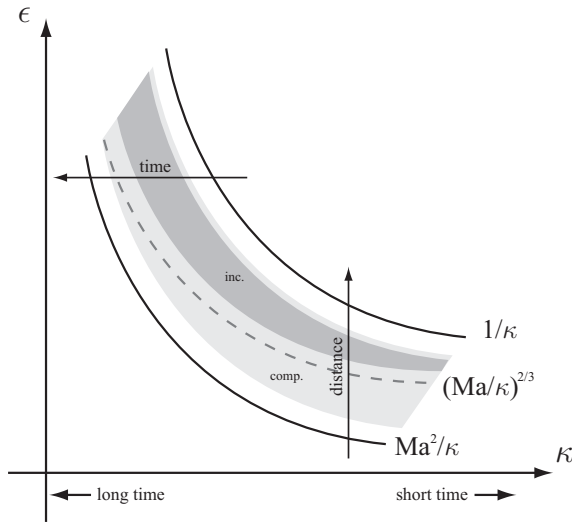


FIG. 3. Regions of validity of the inviscid incompressible (45) (dark shaded) vs the compressible (92) (light shaded) approximations for $\text{Ma} \ll 1$. The time and distance arrows crossing the region indicate the growth of the corresponding variable (time or distance), cf. discussion in Sec. VI.

where $\tilde{\delta} = \delta \text{Ma}/(\epsilon \kappa) = (\text{Ma}/\kappa)/\epsilon^{3/2} \ll 1$ due to (43) and the term $-v_r \partial h/\partial r$ in the kinematic condition is negligible compared to v_θ/r for small interfacial deflections h .

If $0 < \tilde{\delta} \ll 1$ and $\text{We} = \infty$, the first of equations (47) produces the dynamic condition

$$\theta = h(t, r): \quad \frac{\partial \phi}{\partial t} = 0, \quad (48)$$

from where it also follows that $\phi = 0$ after integration along the interface [17] in the context of the linear problem (1)—this is consistent with $p = 0$ at the free surface based on the Cauchy-Lagrange integral (41b). This condition on the velocity potential in the form (6b) is needed for the classical solution (3) to be valid and entails the orthogonality of the free surface to the velocity vectors at the instant of impact (given here in dimensional form):

$$\theta = 0: \quad v_r = 0, \quad v_\theta \sim r^{-1/2}; \quad (49)$$

i.e., the velocity is directed normal to the interface, cf. Fig. 1(b), which should lead to singular $h(t, r)$ near the edge—the intrinsic deficiency of the classical solution (3). Due to (49), from (47b) we find $\partial h/\partial t \rightarrow \infty$ as $r \rightarrow 0$. Thus, the Kutta-Joukowski condition—the tangential departure of the interface from the plate edge—cannot be enforced. If, on the other hand, for $0 < \tilde{\delta} \ll 1$ one formally neglects the right-hand side in the second of equations (47)

$$\theta = h(t, r): \quad \frac{\partial h}{\partial t} = 0, \quad (50)$$

it entails $h \equiv 0$ if the interface was not deflected initially—this, in turn, would imply that the Kutta-Joukowski condition [18] is satisfied automatically due to the tangential departure of the interface. However, the singularity (49) of v_θ in the classical solution shows inconsistency with nondeflected interface $h = 0$.

Finally, in the real physical situation $\tilde{\delta} \neq 0$ and $\text{We} < \infty$, which implies that both compressibility and surface tension need to be taken into account, as will be discussed in detail in Sec. IV D. For the purpose of the present discussion, we just mention that after reducing (47) to a single equation it becomes clear that when $\tilde{\sigma} \tilde{\delta} \sim O(1)$ surface tension effects must be taken into account and thus

the solution (7) is valid only for the distances

$$\epsilon \gg \frac{(\text{Ma}/\kappa)^{2/3}}{\text{We}^{1/3}}. \quad (51)$$

III. SINGULARITY $r \rightarrow 0$: VISCOUS INCOMPRESSIBLE SUBLIMIT

A. On the prediction of $\delta_\epsilon(t)$ and unimportance of nonlinearity

The discussion of the viscous incompressible case in this section supplements and provides a different angle on the problem of incompressible water impact compared to previous work [19]. To develop some intuition on how viscosity may regularize $\delta(t)$ in the pressure-impulse theory, consider the diffusion problem on a half-line, in which the boundary point $x = 0$ gets an initial release of a finite energy at a single instant of time $t = 0$:

$$\frac{\partial u}{\partial t} = \epsilon \frac{\partial^2 u}{\partial x^2}, \quad (52a)$$

$$x = 0, t \geq 0: u(t, 0) = \delta(t), \quad (52b)$$

$$t = 0, x > 0: u(0, x) = 0. \quad (52c)$$

The solution of this problem

$$u(t, x) = \frac{x}{2\sqrt{\pi \epsilon t^3}} e^{-\frac{x^2}{4\epsilon t}} \quad (53)$$

is no longer singular, but in the limit $\epsilon \rightarrow 0$ (or $t \rightarrow 0$) recovers $\delta(t)$. Hence, in our problem, in the presence of viscosity it is natural to expect that $\delta(t)$ in the pressure p and acceleration $\partial \mathbf{v} / \partial t$ is also replaced by a delta sequence $\delta_\epsilon(t)$ with $\epsilon \sim \text{Re}^{-1}$, which in the limit $\text{Re} \rightarrow \infty$ (vanishing viscosity $\nu \rightarrow 0$) gives $\delta(t)$. From physical and characteristics viewpoints [20], the reason for the singular behavior is that the incompressible problem is elliptic, which means that the speed of propagation is infinite—since the effective “front” is propagating as $\sim \sqrt{\nu t}$, its speed $\sim \sqrt{\nu/t}$ is infinite at $t = 0$ [21].

Therefore, in the regularized theory the velocity must have the form $\mathbf{v} \sim H_\epsilon(t) r^n$, where n changes from $-1/2$ in the inviscid region to some positive value in the viscous region to be determined in what follows and $H_\epsilon(t)$ is the Heaviside function smoothed by the viscosity, so that $H'_\epsilon(t) = \delta_\epsilon(t)$ is the delta sequence approximating the Dirac delta function with $\lim_{\epsilon \rightarrow 0} \delta_\epsilon(t) = \delta(t)$. Under such an assumption, one can estimate the terms in the dimensional NSEs as follows:

$$\underbrace{\frac{\partial \mathbf{v}}{\partial t}}_{V_0 \sqrt{\frac{L}{r}} \delta_\epsilon(t)} + \underbrace{(\mathbf{v} \cdot \nabla) \mathbf{v}}_{V_0^2 \frac{1}{r^2}} = - \underbrace{\frac{1}{\rho} \nabla p}_{V_0 \sqrt{\frac{L}{r}} \delta_\epsilon(t)} + \underbrace{\nu \Delta \mathbf{v}}_{\nu V_0 \sqrt{\frac{L}{r}} \frac{1}{r^2}}, \quad (54)$$

where the strongest singularity in space (from the inviscid region) was assumed. Hence, only the first, most singular in time, terms on the left- and right-hand sides in (54) can balance each other, bringing us to (1). An alternative way to appreciate the linear structure of the governing equations at early positive times is first to realize that since Eq. (1) is linear, due to continuity its extension to $t > 0$ must be also linear at leading order up to some finite time: thus, in analogy with the problem (52) one may expect that the Dirac delta function $\delta(t)$ in the solution for the impact on an ideal fluid should be replaced by a delta sequence $\delta_\epsilon(t)$ in the impact on a real fluid, where ϵ represents the physical effect (such as viscosity ν) responsible for smoothing $\delta(t)$. For positive times, $t > 0$, regardless how small, one needs to account for viscosity and hence retain the viscous stresses term $\nabla \cdot \boldsymbol{\tau}$ in (8) in order to satisfy the no-slip boundary condition at the plate. A systematic justification of the above considerations will be given in Sec. III B.

B. Formal analysis

The requirements necessary for the validity of the incompressible viscous approximation include the conditions on

$$\text{importance of viscous terms: } \epsilon \sim \epsilon_{\text{visc}} = \left(\frac{\text{Ma}}{\kappa \text{Re}} \right)^{1/2}, \quad (55a)$$

$$\text{unimportance of nonlinearity: } \frac{\delta \text{Ma}}{\epsilon \kappa} \ll 1, \quad (55b)$$

$$\text{incompressibility: } \epsilon \kappa \ll 1. \quad (55c)$$

Combining these yields

$$\kappa \ll \frac{\text{Re}}{\text{Ma}} \quad \text{and} \quad \delta \ll \left(\frac{\kappa}{\text{Ma Re}} \right)^{1/2} = \frac{1}{\text{Ma}} \left(\frac{\kappa}{\text{Re/Ma}} \right)^{1/2}. \quad (56)$$

As follows from the first expression, the time scale becomes arbitrary in the limit $\text{Ma} \rightarrow 0$. Next, the parameter $\tilde{\sigma}$ in (28) becomes

$$\tilde{\sigma} = \frac{1}{\delta} \frac{\text{Re}}{\text{We}}, \quad (57)$$

from which we conclude that the closer to the edge, $\delta \rightarrow 0$ (obviously), the larger $\tilde{\sigma}$ and hence the contribution of surface tension becomes important.

With these considerations, the *viscous incompressible sublimit* corresponds to the continuity equation (36) and the (nondimensional) viscous stress tensor now reduces to $\boldsymbol{\tau} = \nabla \mathbf{v} + (\nabla \mathbf{v})^\dagger$, so that $\nabla \cdot \boldsymbol{\tau} = \nabla^2 \mathbf{v}$ and the viscous incompressible momentum equation is

$$\frac{\partial \mathbf{v}}{\partial t} = -\nabla p + \nabla^2 \mathbf{v}. \quad (58)$$

The dynamic boundary condition is just (28) or, in component form (29), with ϵ given by (55a) and $\tilde{\sigma}$ by (57).

Historically, self-similarity was the key to understanding the flow structure near the plate edge in both inviscid [22] and viscous [19] incompressible cases. Applying the affine group transformation (the angle coordinate θ is naturally not transformed)

$$t \rightarrow \alpha t, \quad r \rightarrow \beta r, \quad \mathbf{v} \rightarrow \gamma \mathbf{v}, \quad p \rightarrow \zeta p, \quad (59)$$

to the system (36) and (58), where the pressure variable is needed in the incompressible approximation, and determining the conditions on the scaling factors $\alpha, \beta, \gamma, \zeta$ under which this system stays invariant, we find that $\alpha = \beta^2$, $\zeta = \gamma/\beta$, which means that the solution is self-similar [19], i.e., the velocity field has the form $\mathbf{v} \sim t^a \tilde{\mathbf{v}}(\eta)$ with $\eta = r/t^{1/2}$ and some power a . Clearly, this self-similarity is more restrictive than in the inviscid incompressible case: indeed, applying (59) to the system (36) and (39), we find that the only restriction in the latter case is $\gamma = \zeta \alpha / \beta$. We will revisit this discussion in Sec. III C.

To analyze the system (36) and (58), one can introduce the stream function ψ such that

$$v_r = \frac{1}{r} \frac{\partial \psi}{\partial \theta}, \quad v_\theta = -\frac{\partial \psi}{\partial r}, \quad (60)$$

and hence, after applying $\nabla \times$ to the incompressible momentum equation (58), it becomes

$$\frac{\partial}{\partial t} \Delta \psi = \Delta^2 \psi. \quad (61)$$

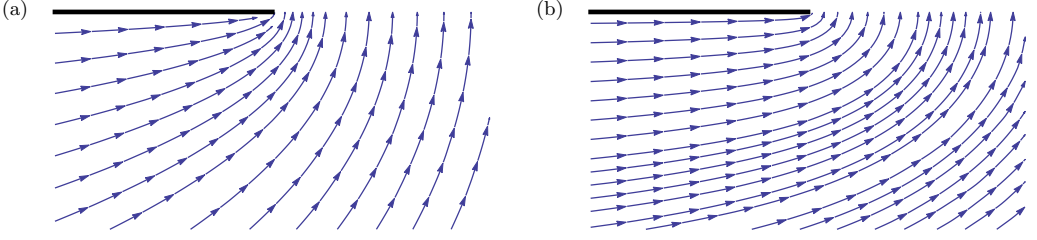


FIG. 4. Inviscid (a) and Stokes (b) streamline patterns near the plate edge in the eigensolution setting (only leading-order terms in the asymptotic expansions (5) and (65) are plotted). In contrast to the Stokes solution where the no-slip condition slows the flow down, the inviscid solution exhibits distinguished crowding of the streamlines near the plate edge, where the velocities are considerable. Viscosity also affects the apparent slope of the streamlines, though in both cases they end up meeting the interface orthogonally.

Finally, the boundary conditions are

$$\text{no-slip: } \theta = -\pi: \quad \psi = \psi_\theta = 0, \quad (62a)$$

$$\text{free boundary: } \theta = 0: \quad \text{Eqs. (28) and (30)}, \quad (62b)$$

where the scalings in (28) and (30) should comply with the considerations at the beginning of this section. Note that while in previous work [19] the solution to the above problem was constructed by first finding self-similarity, and only then taking the limit $t \rightarrow 0$ so that nonlinear terms are neglected, here we first derived the general equation (61) and only then find its self-similar solution, which is apparently a function of a self-similar independent variable $\tilde{r} = \epsilon \kappa^{1/2} \text{Ma}^{-1/2} r / \sqrt{t}$ as (61) is a diffusion-type equation. The time exponent in the self-similar representation of ψ is found from the requirement that we need $\mathbf{v} \sim r^{-1/2}$ in order to be able to match with inviscid asymptotics (4), so that the stream function in the physical space $V_0^{5/4} t^{3/4} \tilde{\psi}(\tilde{r})$ or, after application of (16) and (25), in nondimensional form $\psi = \delta^{-1} \epsilon^{-1} \kappa^{-1/4} \text{Ma}^{1/4} t^{1/4} \tilde{\psi}(\tilde{r})$, where bar denotes dimensional variables and $\tilde{\psi}(\tilde{r})$ is the self-similar dependent variable.

As established in previous work [19], the solution to (61) and (62) uniformly valid in both inviscid and viscous regions can be expressed in terms of confluent hypergeometric functions (for further details the reader is referred to Ref. [19]). Its inviscid asymptotics for $\tilde{r} \gg \epsilon^{1/2}$, where $\epsilon = 2\kappa \epsilon^2 / \text{Ma} = 2/\text{Re}$ is different from ϵ introduced in (55a), reads

$$\tilde{\psi}(\tilde{r}, \theta) = -\frac{C_1}{2} \epsilon \ln \epsilon \tilde{r}^{1/2} \cos \frac{\theta}{2}, \quad (63)$$

which allows us to determine the value of the constant $C_1 = 2\sqrt{2}/(\epsilon \ln \epsilon)$ as there should be no ϵ dependence in the inviscid limit; i.e., the leading-order term is

$$\tilde{\psi}(\tilde{r}, \theta) = A_0 \tilde{r}^{1/2} \cos \frac{\theta}{2}. \quad (64)$$

The corresponding Stokes asymptotics for $\tilde{r} \ll \epsilon^{1/2}$ is

$$\tilde{\psi}(\tilde{r}, \theta) = C^{(c)} \tilde{r}^{5/2} \left[\cos \frac{5\theta}{2} - 5 \cos \frac{\theta}{2} \right], \quad (65)$$

where $C^{(c)} = -C_1/30 = -\sqrt{2}/(15 \epsilon \ln \epsilon)$. The regularity of this Stokes velocity field (cf. Fig. 4(b)) guarantees that the interface obeying (28) and (30) no longer exhibits a singularity, i.e., does not stretch to infinity as predicted by the inviscid incompressible solution.

Clearly, (63) dominates (65) for $\epsilon^{1/2} \ll \tilde{r} \ll |\epsilon \ln \epsilon|^{1/2}$; note that the minimum of $|\epsilon \ln \epsilon|^{1/2}$ is at $\epsilon = e^{-1}$, thus defining a nonvanishing $O(1)$ interval of applicability of the inviscid solution. The leading-order pressure, $\tilde{p} = \text{Ma}^{-1/4} \kappa^{-3/4} t^{3/4} p = \sqrt{2} \ln^{-1} \epsilon \tilde{r}^{1/2} \sin(\theta/2)$, gives the following

formula in physical space:

$$\rho_0 V_0^{5/4} t^{3/4} \tilde{r}^{-3/4} \tilde{p} = \rho V_0 \sqrt{2l} \frac{\tilde{r}^{-1}}{\ln \varepsilon} \tilde{r}^{1/2} \sin \frac{\theta}{2}, \quad (66)$$

i.e., the pressure is singular at $t = 0$ (from this point on dropping the bar for the dimensional variables), which is a consequence of the incompressible flow approximation. This formula is nothing more than the pressure from the classical potential flow solution discussed in the introduction, with the only difference that the Dirac delta function $\delta(t)$ is now replaced by the delta sequence [23] $\delta_\varepsilon(t) = -t^{-1}/\ln \varepsilon$. Since the formula for pressure (66) is uniformly valid in both viscous and inviscid regions, the pressure distribution in space is the same as from the potential flow solution, but its singular time dependence $\delta(t)$ is smoothed by the viscosity producing $\delta_\varepsilon(t)$ such that in the limit of zero viscosity it converges to the Dirac delta function:

$$\lim_{\varepsilon \rightarrow 0} \delta_\varepsilon(t) = \delta(t). \quad (67)$$

Hence, one must recover the inviscid potential solution (3) and the corresponding governing equation (1) when taking the limit $t \rightarrow 0$ in the NSEs in the weak topology sense, i.e., almost everywhere except for an infinitely thin boundary layer, in the same way as the Euler equations are recovered from the NSEs in the limit of zero viscosity [24]. Indeed, based on the definition of the delta sequence (and the Dirac delta function) as a distribution [23]

$$(\delta(t), \varphi(t)) = \varphi(0) \quad (68)$$

for any test function $\varphi \in C_0^\infty$ (i.e., infinitely differentiable and with compact support), one finds

$$(\delta_\varepsilon, \varphi) = -\frac{1}{\ln \varepsilon} \int_{-\tau_1(\varepsilon)}^{\tau_2(\varepsilon)} \frac{\varphi(t)}{t} dt = -\frac{1}{\ln \varepsilon} \int_{-\tau_1(\varepsilon)}^{\tau_2(\varepsilon)} \frac{\varphi(t) - \varphi(0)}{t} dt - \frac{1}{\ln \varepsilon} \int_{-\tau_1(\varepsilon)}^{\tau_2(\varepsilon)} \frac{\varphi(0)}{t} dt, \quad (69)$$

where in the limit $\tau_{1,2}(\varepsilon) \rightarrow 0$ as $\varepsilon \rightarrow 0$ the first integral vanishes since $\varphi(t) - \varphi(0) = O(t)$ as $t \rightarrow 0$ and the second integral gives

$$-\frac{\varphi(0)}{\ln \varepsilon} \ln \frac{\tau_2(\varepsilon)}{\tau_1(\varepsilon)} = \frac{\varphi(0)}{\ln \varepsilon} \ln \frac{\tau_1(\varepsilon)}{\tau_2(\varepsilon)}. \quad (70)$$

That is by appropriately choosing the interval of integration, $\tau_1(\varepsilon)/\tau_2(\varepsilon) = \varepsilon$ as $\varepsilon \rightarrow 0$, one proves that our delta sequence $\delta_\varepsilon(t)$ converges to the Dirac delta function $\delta(t)$, since $\lim_{\varepsilon \rightarrow 0} (\delta_\varepsilon, \varphi) = \varphi(0)$. Note that the asymmetry of the time integration interval $[-\tau_1(\varepsilon), \tau_2(\varepsilon)]$, as opposed to the symmetry of integration limits in Cauchy's principal value method, is dictated by the physical asymmetry of the impact event in time: the fluid is undisturbed for $t < 0$ and disturbed for $t > 0$.

C. On Yakimov's self-similarity

Just to conclude the discussion of the inviscid incompressible solution, let us revisit its self-similar structure, which, as was shown in Sec. III B, admits a continuum of self-similar dependent variables. Let us look at the above mentioned and Yakimov's [22] self-similarities:

$$\text{present: } r \rightarrow t^{1/2} \tilde{r}, \quad \mathbf{v} \rightarrow t^{-1/4} \tilde{\mathbf{v}}, \quad (71a)$$

$$\text{Yakimov's: } r \rightarrow t^{2/3} \tilde{r}, \quad \mathbf{v} \rightarrow t^{-1/3} \tilde{\mathbf{v}}. \quad (71b)$$

Notably, while both scalings give (4), since they are designed based on the asymptotics (4) of the classical potential flow solution, Yakimov's scaling (71b) hinges on the assumption that

$$\mathbf{v} = \frac{d\mathbf{r}}{dt}, \quad (72)$$

which, together with (4), leads to (71b). Formally, this self-similarity is allowed in the inviscid incompressible case, cf. discussion in Sec. III B. However, (72) is the equation for pathlines, i.e., the line traced by a given particle—this is a Lagrangian concept and therefore the application of the Yakimov’s scaling obtained from it to the equations in Eulerian variables is fundamentally flawed. Such an assumption can be valid only if the Lagrangian and Eulerian descriptions coincide, but they are almost always different for unsteady problems: the streamlines and pathlines generally differ in the unsteady case. The problem under consideration is obviously intrinsically unsteady. At the interface, which is a material line, however, each point moves with the same velocity as the fluid thanks to the kinematic boundary condition (11) and thus one arrives at the scaling (71b), which explains why the comparison with experimental measurements of the interfacial motion in Peters *et al.* [25] is in reasonable agreement with Yakimov’s scaling. As for the whole flow [19], Yakimov’s scaling (71b) fails to preserve the property that “in the limit $t \rightarrow 0$ in the Navier-Stokes equations one must recover (1) and the corresponding inviscid potential solution (3)” (p. 7 of Ref. [19]) after the self-similar scaling is applied to the NSEs, since in general self-similarity simply limits the possible solutions of the corresponding PDE to a more narrow class (cf. Appendix B).

IV. SINGULARITY $t \rightarrow 0$: INVISCID WEAKLY COMPRESSIBLE SUBLIMIT

After the mentioned earlier work of von Karman [1], the first significant quantitative advancement in understanding compressible effects was made by Galin [26], who used the displacement potential formulation [27] along with some results from supersonic aerodynamics [28], allowing him to obtain the formula for the time-dependent force acting on the impacting plate of half-length l during the times $0 < t < l/c_0$ and to predict rebound phenomena under certain conditions. Later, in the velocity potential formulation, Flitman [29] and Mikhlin [30] analyzed the same problem, and Ogilvie [31] extended Galin’s analysis for later times. Equivalently, the same problem of compressible impact in the potential flow formulation can be solved in terms of the pressure variable, which was done by Kubenko [32] and Sagomonian [33].

A. Weakly compressible limit

From the scaled continuity equation (26), it follows that in order to get its weakly compressible limit

$$\frac{\partial \rho}{\partial t} + \nabla \cdot \mathbf{v} = 0, \quad (73)$$

one should require $[\delta \text{Ma}/\epsilon] \kappa^{-1} \Delta^{-1} \sim 1$ along with $\Delta \ll 1$, which together with (32) and (34) produces a Ma-independent condition

$$\epsilon \sim \kappa^{-1}, \quad (74)$$

which makes sense as the wave equation $\partial_t^2 \sim \partial_x^2$, after applying the scalings (25), implies that $\kappa \sim \epsilon^{-1}$ as required to resolve the shock-wave region. As follows from (35) and (74), the nonlinear terms can be neglected provided

$$\delta \text{Ma} \ll 1. \quad (75)$$

Altogether, the *inviscid weakly compressible sublimit* corresponds to

$$\frac{\partial p}{\partial t} + \nabla \cdot \mathbf{v} = 0, \quad (76a)$$

$$\frac{\partial \mathbf{v}}{\partial t} = -\nabla p, \quad (76b)$$

where we took into account that $\partial\rho/\partial t = (d\rho/dp) \partial p/\partial t$ with $d\rho/dp = 1$ in the scaled variables (16) and (25). In the case of potential flow, i.e., when $\mathbf{v} = \nabla\phi$, (76) reduces to

$$\frac{\partial^2\phi}{\partial t^2} = \Delta\phi, \quad (77a)$$

$$p = -\frac{\partial\phi}{\partial t}, \quad (77b)$$

where the latter equation is again the Cauchy-Lagrange integral. At the interface, we get from (77b) and (30)

$$\theta = h(t,r): \quad \frac{\partial\phi}{\partial t} = -\tilde{\sigma} \nabla \cdot \mathbf{n}, \quad (78a)$$

$$\frac{\partial h}{\partial t} = \tilde{\delta} \left(-v_r \frac{\partial h}{\partial r} + \frac{v_\theta}{r} \right). \quad (78b)$$

If $We = \infty$ (surface tension is not important), we get the classical case $\partial\phi/\partial t|_{\theta=h} = 0$ from where it follows that $\phi|_{\theta=h} \approx 0$ based on the same considerations as in Sec. IID. In general, surface tension is important when $\tilde{\sigma} \tilde{\delta} = O(1)$ as can be seen by reducing (78) to a single equation.

B. Compressible inviscid solution: global problem and resolution of the singularity $t \rightarrow 0$

Based on the above considerations, the global problem statement for the impact of a finite plate in absence of surface tension is

$$y < 0: \quad (\text{bulk}): \quad \frac{\partial^2\phi}{\partial t^2} = \Delta\phi, \quad (79a)$$

$$t = 0: \quad \phi = \phi_t = 0, \quad (79b)$$

$$y = 0: \quad (\text{plate}): \quad \frac{\partial\phi}{\partial y} = -1, \quad |x| < 1, \quad (79c)$$

$$(\text{free surface}): \quad \phi(t,x) = 0, \quad |x| > 1, \quad (79d)$$

where the initial condition (79b) represents the fact that due to the finite speed of signal propagation the fluid is undisturbed right at the moment of impact. The solution to (79) in the entire lower half-plane is formally determined from

$$\phi(t,x,y) = \frac{1}{\pi} \iint_{\Xi} \frac{w(\tau,\xi) d\tau d\xi}{\sqrt{(t-\tau)^2 - (x-\xi)^2 - y^2}}, \quad (80)$$

where the region of integration Ξ is defined in Fig. 5 and the function $w(t,x) = \partial\phi/\partial y|_{y=0}$ is known only at the plate surface, $w(t,x) = -1$ for $|x| \leq 1$, while for $|x| > 1$ it needs to be found from the integral equation

$$\frac{1}{\pi} \iint_{\Xi} \frac{w(\tau,\xi) d\tau d\xi}{\sqrt{(t-\tau)^2 - (x-\xi)^2}} = 0. \quad (81)$$

The solution of (81) is [29]

$$w(t,x) = \begin{cases} 0, & x > t, \\ \frac{2}{\pi} \left[\arccos \sqrt{\frac{x}{t}} - \sqrt{\frac{t}{x} - 1} \right], & x < t, \end{cases} \quad (82)$$

which has a singularity $w(t,x) \sim 1/\sqrt{x}$ as $x \rightarrow 0$.

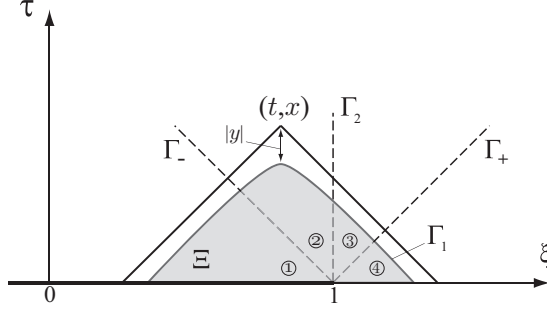


FIG. 5. The domain of integration σ in (80) and the regions (1–4) of the solution definition. Region σ (shaded) is bounded below by the ξ axis and above by the curve $\Gamma_1: \tau = t - \sqrt{(x - \xi)^2 + y^2}$. Regions 1–4 are separated by the ξ axis, the trajectory of the plate edge $\Gamma_2: |\xi| = 1$, and the characteristics $\Gamma_{\pm}: \xi - 1 = \pm\tau$. The plate corresponds to the points $|\xi| \leq 1$.

Given the knowledge of the function $w(t, x)$ everywhere on the x axis, the solution to (79) can be expressed as

$$\phi(t, x, y) = -\frac{t}{2} + \frac{1}{\pi} \int_0^t \arcsin \frac{x - 1 + \tau - \sqrt{(x - 1)^2 + y^2}}{\sqrt{\tau^2 - y^2}} d\tau \quad (83)$$

and is weakly discontinuous (i.e., continuous itself but has discontinuous derivatives): snapshots in time are shown in Fig. 6. While (83) admits explicit integration in terms of elementary functions, for the sake of brevity we will refer only to this integral representation. Also, note that pressure can be readily found from (83) via $p = -\phi_t$. In the compressible inviscid case, obviously pressure is no longer a Dirac delta function at $t = 0$, i.e., the force which acts on the plate is finite, consistent with the work of Galin [26].

C. Relaxation to inviscid incompressible solution without surface tension

To understand how the inviscid compressible solution (83) relaxes to the incompressible one (7) near the plate edge, let us consider the limit $t \gg r$ corresponding to the solution behind the shock wave (or $\epsilon \ll \kappa^{-1}$ after (25) is applied). In this case, the integrand in (83) simplifies to

$$\arcsin \frac{x - 1 + \tau - \sqrt{(x - 1)^2 + y^2}}{\sqrt{\tau^2 - y^2}} \simeq \arcsin \frac{1 - 2 \sin^2 \frac{\theta}{2}}{t/r} \simeq \frac{\pi}{2} - \frac{2 \sin \frac{\theta}{2}}{\sqrt{t/r}}, \quad (84)$$

so that the velocity potential becomes

$$\phi(t, r, \theta) = -\frac{4}{\pi} \sin \frac{\theta}{2} r^{1/2} t^{1/2}. \quad (85)$$

One can arrive at this asymptotic solution independently, without knowledge of the complete global solution (83), which also helps to highlight its physical significance. Given the problem statement defined by the eigenproblem (79a) and (6), we can look for a local compressible inviscid solution. The idea is that the form of the inviscid incompressible solution (7) should stay relevant after the compression wave passed, $t \gg r$, so that we can expect the following form:

$$\phi = \text{const } t^m r^{1/2} \sin \frac{\theta}{2}, \quad (86)$$

which makes the Laplacian part of the wave equation (79a) vanish. This means that time dependence should be determined from some other principles (note that we dropped the initial conditions (79b) since the solution is considered for $t \gg r$; this solution construction procedure can also be reconciled

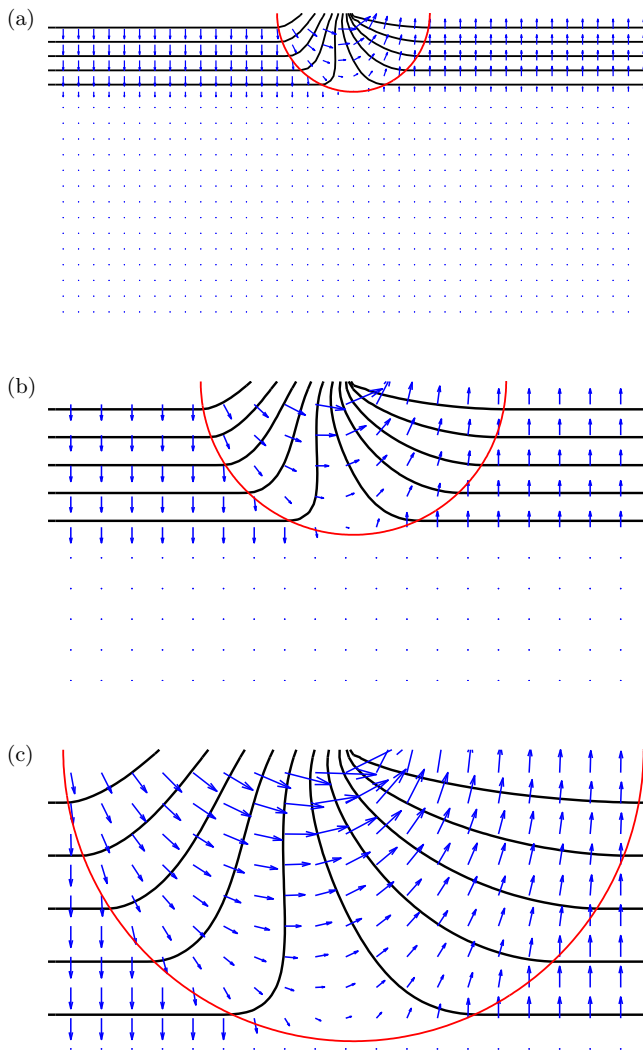


FIG. 6. Equipotential patterns (black lines) of (83) and velocity fields (blue arrows) near the plate edge at three different times: (a) $t = t_1 \ll l/c_0$, (b) $t = 2t_1$, and (c) $t = 4t_1$; the half-circle shows the boundary of the disturbance and its center corresponds to the plate edge. The scaling self-similarity of panels (a)–(c) suggests self-similarity of the solution near the edge at early times.

by a recursive approach, cf. Appendix D). Physically, $t \gg r$ means that we are studying decay (the tail) of the signal after the compression wave has passed. Since the pressure and the velocity potential are related via $\int dp/\rho = -\phi_t$ and one can view the plate edge as an instantaneous source of energy, which creates the compression (strong shock, in the high energy case) wave, in such a situation pressure is known to decay as

$$p \sim t^{-1/2} \quad (87)$$

after the propagation of a cylindrical shock wave produced by an instantaneous energy release from a line source [34]; hence the exponent in (86) is $m = 1/2$. This theory is an extension of Taylor's original work [35] on an atomic explosion in the atmosphere from spherical geometry to the cylindrical one [36] in the case when the shock propagation and its speed depend on the equation of state, such as

in the underwater explosion [34,37,38]. In our case, however, weak compressibility is considered, which brings us to the linear wave equation (79a) and hence the compression (shock) wave speed is that of sound. Notably, (87) shows that the role of compressibility (liquid elasticity) is in the slower relaxation of pressure compared to $p \sim \delta(t)$ in the classical pressure-impulse theory, where pressure impulse relaxes sharply for $t > 0$. Another way to view (86) with $m = 1/2$ is by taking into account that the solution to (79) near the plate edge is self-similar (after applying the affine scaling (59) we find that $\alpha = \beta$):

$$\phi \sim t \Phi(\eta, \theta), \quad \eta = r/t, \quad (88)$$

based on the symmetry of the wave equation (79a) and the boundary conditions (6)—the eigenvalue solution corresponds to the choice of the power a in $\phi \sim t^a \Phi(\eta, \theta)$ which gives the same leading-order nondegenerate solution as in the incompressible case [8] (cf. Appendix C). The solution (85) can also be constructed using the Laplace transform method (cf. Appendix E).

The global solution (cf. Sec. IV B) allows one to establish the value of the factor in (86), which is $-4/\pi$ valid for $t \gg r$, i.e., after the compression wave passed. In summary, after propagation of the compression wave the solution “relaxes” back to the inviscid incompressible solution (7): compare Figs. 4(a) and 6. As a result, the solution (85) does not allow one to take the limit $t \rightarrow 0$ for a fixed r since when $t \sim r$ the asymptotics becomes invalid and should correspond to the compression wave, while for $t < r$ the solution becomes zero (in the inviscid approximation) as the shock wave has not propagated yet. However, in the viscous approximation the solution is nonzero even for $t < r$, which will be elaborated on in Sec. V.

Applying the scalings (16) and (25) to (85) consecutively, we find the scaling for velocity

$$\delta \sim \epsilon^{-1/2} \kappa^{-1/2}, \quad (89)$$

which is valid provided $\epsilon \ll \kappa^{-1}$. This means that in this limit (behind the shock wave)

$$\delta \gg 1, \quad (90)$$

which is expected as the solution should relax to the incompressible one (42) singular near the plate edge. Given (89), the nonlinear terms are negligible, as per (75), provided

$$\epsilon \gg \text{Ma}^2/\kappa, \quad (91)$$

where clearly one needs $\kappa \gg \text{Ma}^2$ (long time limit) as ϵ must be small. Altogether, solution (85) is valid provided

$$\text{Ma}^2/\kappa \ll \epsilon \ll \kappa^{-1} \ll \text{Ma}^{-2} \quad (92)$$

versus the analogous condition (45) in the incompressible case, cf. Fig. 3. Thus, nonlinearity in the compressible case becomes important if $\epsilon \sim \text{Ma}^2/\kappa$, i.e., close enough to the edge (the shorter the time, i.e., the larger κ , the smaller this distance). Curves κ^{-1} and Ma^2/κ apparently cannot intersect, while the curves Ma^2/κ and $(\text{Ma}/\kappa)^{2/3}$ intersect at $\kappa = \text{Ma}^4$, so that $\epsilon = \text{Ma}^{-2}$; however, one needs $\kappa \gg \text{Ma}^2$ for the solution (85) to be valid as per (92), so such an intersection is not possible.

Turning our attention to the boundary conditions (78) at the interface, with (89) the parameter $\tilde{\delta}$ in (78b) becomes

$$\tilde{\delta} = \frac{\delta \text{Ma}}{\epsilon \kappa} = \left(\frac{\text{Ma}^2/\kappa}{\epsilon} \right)^{3/2} \frac{1}{\text{Ma}^2}, \quad \text{where} \quad \frac{\text{Ma}^2/\kappa}{\epsilon} \ll 1. \quad (93)$$

The parameter $\tilde{\sigma}$ in (78a) can be put in the form

$$\tilde{\sigma} = \left(\frac{\text{Ma}^2/\kappa}{\epsilon} \right)^{1/2} \frac{1}{\epsilon} \frac{1}{\text{We}}, \quad \text{where} \quad \frac{\text{Ma}^2/\kappa}{\epsilon} \ll 1, \quad (94)$$

but, because $\epsilon \ll 1$, the closer to the edge, the more important is surface tension. In fact, there is a (short) distance close enough to the edge $\epsilon \sim (\text{Ma}/\kappa)^{2/3}/\text{We}^{1/3}$ (same as in the incompressible case,

cf. Sec. IID), at which surface tension is no longer non-negligible. Note that (91) can still hold while $\tilde{\sigma} \tilde{\delta}$ becomes $O(1)$ for small enough ϵ as follows from (93) and (94). Altogether, the solution (85) is valid when surface tension effects can be neglected (51) as the boundary condition (78a) should become $\partial\phi/\partial t = 0$, so that $\phi = 0$ on the interface (79d).

D. Post shock wave asymptotics with surface tension

Given the above point that close enough to the plate edge surface tension becomes important, let us consider the post shock wave asymptotics by taking into account surface tension in problem (79). Then instead of condition (79d) we should use (78), where in (78b) we neglect the term $v_r \partial h/\partial r$ based on the same considerations as in the inviscid incompressible case (Sec. IID) since the horizontal velocity component vanishes at $\theta = 0$, cf. (85). The idea is to determine the post shock (long-time) asymptotics with the help of the final value theorem in the Laplace transform theory [4] exemplified in Appendix E for the case of no surface tension. Following the approach of Appendix E and applying the Laplace transform in time to Eq. (78) linearized around $\theta = 0$ we get

$$\theta = 0: \quad \tilde{\sigma} (2\hat{h}_r + r\hat{h}_{rr}) = \lambda\hat{\phi}, \quad (95a)$$

$$\lambda\hat{h} = \frac{\tilde{\delta}}{r^2} \frac{\partial\hat{\phi}}{\partial\theta}. \quad (95b)$$

From the solution of Bessel's equation for small r , cf. Appendix E, we know that $\hat{\phi} = C(\theta)(\lambda r)^n$, so that the first (dynamic) equation above gives

$$\hat{h} = \frac{C(0)}{\tilde{\sigma}(n+1)(n+2)} (\lambda r)^{n+1} \quad \text{for } n \neq -1, -2. \quad (96)$$

The second (kinematic) equation (95b) yields in turn

$$\frac{1}{(n+1)(n+2)} \lambda^2 r^3 C(0) = \tilde{\sigma} \tilde{\delta} C'(0), \quad (97)$$

where $\lambda r \ll 1$ since we are interested in the asymptotics behind the shock wave, i.e., $t \gg r$, which in the Laplace space variable implies $\lambda^{-1} \gg r$. If $\tilde{\sigma} = 0$, then $C(0) = 0$ as in the case considered in the previous section without surface tension. If $\tilde{\sigma} \neq 0$, then without loss assuming that $\tilde{\sigma} \tilde{\delta} = O(1)$, the only reasonable option left is to consider $C'(0) = 0$, which leads to quantization different from the case without surface tension, namely

$$C(\theta) = \text{const} \cos n\theta, \quad n \in \mathbb{Z}. \quad (98)$$

Note that $C'(0) = 0$ implies that the angular velocity v_θ vanishes at the interface (surface tension "rigidifies" the interface) versus $C(0) = 0$ for the classical case $We = \infty$ considered in the previous section. Hence, compressibility (as opposed to incompressibility) does not push the fluid upward at this early stage—this is how compressibility and surface tension regularize the free surface behavior. Since the case $n = 0$ gives a trivial solution, the lowest positive n leading to a nontrivial solution is $n = 1$, i.e., the velocity field $\mathbf{v} = \nabla\phi$ is no longer singular. The basic physical interpretation of this result is that surface tension regularizes the flow near the plate edge, essentially by suppressing it even in absence of viscosity.

V. SINGULARITIES $r \rightarrow 0$ AND $t \rightarrow 0$: VISCOUS WEAKLY COMPRESSIBLE SUBLIMIT

The *viscous weakly compressible sublimit* corresponds to

$$\frac{\partial\rho}{\partial t} + \nabla \cdot \mathbf{v} = 0, \quad (99a)$$

$$\frac{\partial\mathbf{v}}{\partial t} = -\nabla p + \frac{1}{\kappa \epsilon^2} \frac{\text{Ma}}{\text{Re}} \nabla \cdot \boldsymbol{\tau}, \quad (99b)$$

where

$$\nabla \cdot \boldsymbol{\tau} = \Delta \mathbf{v} + \chi \nabla(\nabla \cdot \mathbf{v}), \quad (100)$$

as per (18) and the most nondegenerate case is when $\text{Ma}/(\kappa \epsilon^2 \text{Re}) \sim O(1)$, but we keep it general for now. Applying the affine group transformation (the angle coordinate θ is naturally not being transformed)

$$t \rightarrow \alpha t, \quad r \rightarrow \beta r, \quad \mathbf{v} \rightarrow \gamma \mathbf{v}, \quad p \rightarrow \zeta p, \quad \rho \rightarrow \xi \rho \quad (101)$$

to system (99) and determining the conditions on the scaling factors $\alpha, \beta, \gamma, \zeta, \xi$ under which (99) stays invariant, we find that $\alpha = \beta = 1, \gamma = \xi$, implying that no self-similarity is present. Thus, the analysis of the viscous compressible case is complicated by the absence of a symmetry even though near the plate edge there is no characteristic geometric length scale. This means that for the existence of self-similarities it is not sufficient to have only the absence of an independent geometric length scale (near the edge there is none). Therefore, one can get self-similarities only in the sense of intermediate asymptotics [39], e.g., when one of the effects (compressibility or viscosity) is dominating the other.

A. Irrotational and solenoidal components

The last term in (100) has the meaning of the gradient of the velocity divergence, i.e., it measures how compressibility varies with respect to a particular direction and can be decomposed into

$$\nabla(\nabla \cdot \mathbf{v}) = \Delta \mathbf{v} + \nabla \times \boldsymbol{\omega}, \quad (102)$$

where $\boldsymbol{\omega} = \nabla \times \mathbf{v}$ is the vorticity and the term $\nabla \times \boldsymbol{\omega}$ is called the flexion field [40], which is nonzero even in the 2D case considered here. Using the Helmholtz decomposition theorem [41], we can resolve the velocity field outside the singular point ($r = 0$) into the sum of an irrotational (curl-free) scalar field ϕ and a solenoidal (divergence-free) vector field \mathbf{A} :

$$\mathbf{v} = \nabla \phi + \nabla \times \mathbf{A}, \quad (103)$$

respectively, where ϕ is a scalar potential and \mathbf{A} is a vector potential, which in our 2D case is simply $\mathbf{A} = \psi \mathbf{e}_z$ with some scalar ψ to be defined later and \mathbf{e}_z being the unit vector orthogonal to the plane of motion.

The *first* observation to make is that the compressibility measured by $\nabla \cdot \mathbf{v}$ is contributed only by the irrotational part ϕ of \mathbf{v} since the solenoidal part \mathbf{A} vanishes after the application of the divergence operation

$$\nabla \cdot \mathbf{v} = \nabla^2 \phi + \nabla \cdot (\nabla \times \mathbf{A}) = \nabla^2 \phi = \Delta \phi = -\frac{\partial \rho}{\partial t} \quad (104)$$

in nondimensional variables (16). From (104), we also find that (102) is simply

$$\nabla(\nabla \cdot \mathbf{v}) = \nabla(\Delta \phi). \quad (105)$$

Second, by taking the divergence of the momentum equation (100) and excluding the velocity divergence $\nabla \cdot \mathbf{v}$ using the continuity equation, we get decoupled equations for the density and the

velocity vector:

$$\frac{\partial^2 \rho}{\partial t^2} = \frac{1}{\epsilon^2 \kappa^2} \left[1 + \kappa \frac{\text{Ma}}{\text{Re}} (\chi + 1) \frac{\partial}{\partial t} \right] \Delta \rho, \quad (106a)$$

$$\frac{\partial^2 \mathbf{v}}{\partial t^2} = \frac{1}{\epsilon^2 \kappa^2} \left[1 + \kappa \frac{\text{Ma}}{\text{Re}} \chi \frac{\partial}{\partial t} \right] \nabla (\nabla \cdot \mathbf{v}) + \kappa \frac{\text{Ma}}{\text{Re}} \frac{1}{\epsilon^2 \kappa^2} \frac{\partial}{\partial t} \Delta \mathbf{v}, \quad (106b)$$

respectively. That is, the velocity components are coupled through the flexion field $\nabla \times \boldsymbol{\omega}$ because of (102), so that when the flow is potential (and thus irrotational) the velocity components decouple and obey the standard wave equation for $\text{Re} = \infty$. Both (106a) and (106b) reduce to the wave equation in the limit of $\text{Re} = \infty$ and initially irrotational flow (so that the vorticity $\boldsymbol{\omega}$ vanishes and thus $\nabla (\nabla \cdot \mathbf{v})$ reduces to $\Delta \mathbf{v}$); the additional terms in (106) due to the presence of viscosity account for dissipation. Remarkably, the coupled equations for the velocity components (106b) can be reduced to a scalar equation for the velocity divergence $\nabla \cdot \mathbf{v}$ identical to (106a) for the density:

$$\frac{\partial^2 (\nabla \cdot \mathbf{v})}{\partial t^2} = \frac{1}{\epsilon^2 \kappa^2} \left[1 + \kappa \frac{\text{Ma}}{\text{Re}} (\chi + 1) \frac{\partial}{\partial t} \right] \Delta (\nabla \cdot \mathbf{v}), \quad (107)$$

which shows how the quantity $\nabla \cdot \mathbf{v} = -\partial \rho / \partial t$ evolves in time; note that (107) gives an equation for $\Delta \phi$ from (104).

Third, the equation for the vorticity evolution is obtained by taking the curl of the momentum equation (99), producing the diffusion equation

$$\frac{\partial \boldsymbol{\omega}}{\partial t} = \frac{1}{\kappa \epsilon^2} \frac{\text{Ma}}{\text{Re}} \Delta \boldsymbol{\omega}, \quad (108)$$

where $\boldsymbol{\omega}$ has only one component in 2D, i.e., in the \mathbf{e}_z direction, so that (108) is scalar in essence. Equations (107) and (108) also form a closed system, but decoupled as opposed to the vector equation (106b). Taking into account that in 2D the vorticity is expressed as $\boldsymbol{\omega} = \nabla \times \mathbf{v} = -\Delta \mathbf{A}$ and $\mathbf{A} = \psi \mathbf{e}_z$, one can rewrite (108) for the stream function ψ :

$$\frac{\partial}{\partial t} \Delta \psi = \frac{1}{\kappa \epsilon^2} \frac{\text{Ma}}{\text{Re}} \Delta^2 \psi. \quad (109)$$

The velocity vector (103) can then be found from the knowledge of $\nabla \cdot \mathbf{v}$ and $\nabla \times \mathbf{v}$ after solving (107) and (108), respectively, since $\phi = \Delta^{-1} (\nabla \cdot \mathbf{v})$ and $\mathbf{A} = -\Delta^{-1} \boldsymbol{\omega}$.

The above discussion of the irrotational and solenoidal components of the solution allows one to reach an important conclusion. Namely, as follows from Eqs. (107) and (108), the irrotational ϕ part evolves according to the wave equation (hyperbolic), while the solenoidal \mathbf{A} part evolves according to the diffusion equation (parabolic). As we will see, these two processes are important for understanding the interplay of compressible and viscous effects in the resolution of the pressure-impulse theory singularities and can be related to the characteristic analysis of (99) to be performed next, in Sec. VB. Finally, note that in general both components in (103) are nonzero at the interface and hence the vorticity is important in understanding the interface evolution.

B. Characteristic analysis and the physics behind it

Performing a change of independent variables to the characteristic surface [42] $(t, r) \rightarrow \Omega(t, r)$ in (99) converted back to dimensional variables in order to highlight the physics of the signal propagation processes, we find the following determinant defining the characteristic surface $\Omega(t, r)$:

$$\begin{vmatrix} \rho_0 \Omega_r & \rho_0 \Omega_r & \Omega_t \\ \rho_0 \Omega_t - \mu \Omega_r^2 - \left(\lambda + \frac{\mu}{3} \right) \Omega_r^2 & -\left(\lambda + \frac{\mu}{3} \right) \Omega_r^2 & c_0^2 \Omega_r \\ -\left(\lambda + \frac{\mu}{3} \right) \Omega_r^2 & \rho_0 \Omega_t - \mu \Omega_r^2 - \left(\lambda + \frac{\mu}{3} \right) \Omega_r^2 & c_0^2 \Omega_r \end{vmatrix} \\ = \left\{ \rho_0 \Omega_t - \mu \Omega_r^2 \right\} \left\{ \rho_0 \Omega_t^2 - \Omega_r^2 \left[\rho_0 c_0^2 + \left(\lambda + \frac{4\mu}{3} \right) \Omega_t \right] \right\} = 0, \quad (110)$$

where the first bracket on the right clearly stands for the parabolic behavior, while the second bracket gives both hyperbolic (nondissipative terms) with a finite speed of propagation $c_0 = \pm\Omega_r/\Omega_r$ and parabolic behavior (dissipative terms). The analysis above is done for simplicity in the polar system of coordinates, since we are interested in propagation of information along \mathbf{e}_r . Note that the original NSEs (8) have the same characteristic properties.

The mixed characteristic type of the system (99) has a simple physical explanation, which will be crucial for our further considerations. Namely, over the time t since the moment of impact, viscous effects (due to the initial wall jet propagating from the high-pressure region at the plate center to the plate edge where the pressure is atmospheric) diffuse a distance $l_v = \sqrt{\nu t}$ and the compressible effects propagate a distance $l_c = c_0 t$. Due to the difference in the time exponents, this observation implies that up to the time

$$t_* = \mu/(\rho_0 c_0^2), \quad (111)$$

and thus the distance

$$l_* = \mu/(\rho_0 c_0), \quad (112)$$

viscous effects propagate faster and, in fact, the speed of propagation at $t = 0$ is infinite as is common in parabolic systems. This interesting property of the compressible viscous NSEs allows for their (equations') regularization at short times. For $t > t_*$, a compression wave propagates in the inviscid region, but, of course, the compression wave itself is regularized by viscosity locally [43–45]. It is notable that both t_* and l_* depend only on the fluid properties. For example, using values from Ref. [46], for water one finds $t_* = 10^{-12}$ s and $l_* = 10^{-9}$ m, while for glycerol $t_* = 10^{-9}$ s and $l_* = 10^{-6}$ m. The expressions (111) and (112) show that under certain conditions such as for water at atmospheric pressure and room temperature the characteristic scales are at the limits of the continuum description and therefore require insights into new physical phenomena not accounted in the NSEs (cf. Appendix F).

To get a better understanding of the physical meaning of t_* and l_* , recall that, compared to gases and solids, interactions in liquids are both system specific and strong [47,48] and therefore maintain modes with wavelengths ranging from the body size down to interatomic separations [49]. As argued by Frenkel [47], liquid flow results from thermally activated spatial rearrangement of atoms (or molecules), which are not fixed, but may jump from their surrounding cage, accompanied by large-scale rearrangement of the cage atoms—this process corresponds to each flow event and is called a local relaxation with the associated time τ between these events at one point in space estimated as μ/G , where G is the instantaneous shear modulus [50]. In this context, it must be noted that the time scale t_* estimated above (111) is comparable to the characteristic relaxation time scale τ of liquid matter [47] below which liquids behave like solids, since $t_* \sim \mu/K$, where K is the bulk modulus typically of the same order as the shear modulus G [46]. This fact in turn affects the interpretation of both the diffusion mechanisms (phonon vs nonphonon propagation) and sound propagation since solids maintain not only longitudinal waves but also transverse waves—the latter are absent in liquids and gases under normal conditions. However, on the time scales below t_* liquids exhibit elastic shear stresses opposing deformations similar to solids, while under the normal conditions, $t \gg t_*$, liquids (or any other fluids, for that matter) do not oppose resistance to shear forces but only to rate of shear deformations.

Based on the above characteristic analysis and the discussion in Sec. V A, one arrives at the flow structure shown in Figs. 7(a) and 7(b), when the viscous front could be faster than the shock wave and the opposite, respectively. In Fig. 7(a), the shock wave is propagating in the region already affected by viscous diffusion, while in Fig. 7(b) there is region 3, which is inviscid and affected by compressibility due to the propagated shock wave, separating the viscous region 1 and the shock wave 2, which is, of course, regularized by viscous effects. Hence, the competing diffusion and shock wave propagation effects dictate the solution structure.

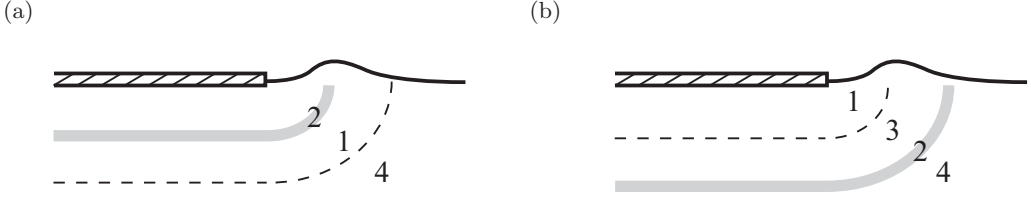


FIG. 7. On the flow structure: (a) $c_0 t < \sqrt{v t}$, (b) $c_0 t > \sqrt{v t}$. Dashed line is the “viscous front” $\sqrt{v t}$; solid line is the shock wave $c_0 t$. Regions: 1—affected by viscous diffusion, 2—viscosity smoothed shock wave, 3—unaffected (yet) by viscous diffusion, 4—undisturbed (quiescent) fluid.

C. Early-time limit

As follows from the structure of Eq. (106b), it is not separable in general. However, by rewriting it in the form

$$\epsilon^2 \kappa^2 \frac{\text{Re}}{\kappa \text{Ma}} \frac{\partial^2 \mathbf{v}}{\partial t^2} = \left[\frac{\text{Re}}{\kappa \text{Ma}} + \chi \frac{\partial}{\partial t} \right] \nabla (\nabla \cdot \mathbf{v}) + \frac{\partial}{\partial t} \Delta \mathbf{v}, \quad (113)$$

we can see that in the limit of early time, $\kappa \rightarrow \infty$, while $\epsilon \kappa \sim O(1)$ so that $\epsilon \rightarrow 0$ (close to the plate edge), we are left with the diffusion part only (since for short times $\sim \sqrt{t}$ grows faster than $\sim t$ and hence the wave equation component $\mathbf{v}_{tt} \sim \Delta \mathbf{v}$ is negligible):

$$\chi \frac{\partial}{\partial t} \nabla (\nabla \cdot \mathbf{v}) + \frac{\partial}{\partial t} \Delta \mathbf{v} = 0. \quad (114)$$

The latter is also not separable in general, but becomes so in the vicinity of the plate edge $\mathbf{v} \sim r^n$ for $r \rightarrow 0$; as for values of χ we consider the interval $\chi \in [1/3, 1]$, i.e., $\lambda/\mu \in [0, 2/3]$. Integrating Eq. (114) with respect to time and without loss taking the constant of integration (function of space) to be zero, we get $\chi \nabla (\nabla \cdot \mathbf{v}) + \Delta \mathbf{v} = 0$ or in component form

$$\frac{1}{r} \frac{\partial}{\partial r} \left(r \frac{\partial v_r}{\partial r} \right) + \frac{1}{r^2} \frac{\partial^2 v_r}{\partial \theta^2} + \chi \frac{\partial}{\partial r} \left[\frac{1}{r} \frac{\partial}{\partial r} (r v_r) + \frac{1}{r} \frac{\partial v_\theta}{\partial \theta} \right] = 0, \quad (115a)$$

$$\frac{1}{r} \frac{\partial}{\partial r} \left(r \frac{\partial v_\theta}{\partial r} \right) + \frac{1}{r^2} \frac{\partial^2 v_\theta}{\partial \theta^2} + \chi \frac{1}{r} \frac{\partial}{\partial \theta} \left[\frac{1}{r} \frac{\partial}{\partial r} (r v_r) + \frac{1}{r} \frac{\partial v_\theta}{\partial \theta} \right] = 0. \quad (115b)$$

These equations are supplied with the no-slip boundary conditions at the plate,

$$\theta = -\pi: \quad v_r = v_\theta = 0, \quad (116)$$

and the following conditions at the interface. Assuming that the interfacial deflection from flat interface is small for early times and close to the edge, so that $\mathbf{n} \simeq \mathbf{e}_\theta$ and $\mathbf{t} \simeq \mathbf{e}_r$, we get the set of boundary conditions linearized around $\theta = 0$:

$$\text{tangential: } \frac{1}{r} \left(\frac{\partial v_r}{\partial \theta} - v_\theta \right) + \frac{\partial v_\theta}{\partial r} = 0, \quad (117a)$$

$$\text{normal: } \frac{2}{r} \left(\frac{\partial v_\theta}{\partial \theta} + v_r \right) + \frac{\chi - 1}{r} \left[\frac{\partial}{\partial r} (r v_r) + \frac{\partial v_\theta}{\partial \theta} \right] = \frac{1}{\delta} \frac{\text{Re}}{\text{We}} [2 h_r + r h_{rr}], \quad (117b)$$

$$\text{kinematic: } \frac{\partial h}{\partial t} = \delta \text{Ma} \frac{v_\theta}{r}. \quad (117c)$$

Note that (117b) follows from (29a), first rewritten as

$$\theta = h(t, r): \quad \mathbf{n}: \quad p - \frac{1}{\kappa^2 \epsilon^2} \frac{\kappa \text{Ma}}{\text{Re}} \mathbf{n} \cdot \boldsymbol{\tau} \cdot \mathbf{n} = \frac{\kappa \text{Ma} / \text{We}}{\delta \kappa^2 \epsilon^2} \nabla \cdot \mathbf{n}, \quad (118)$$

then plugging (74) in and taking the limit $\kappa \rightarrow \infty$ in

$$\theta = h(t, r): \quad \mathbf{n}: \quad \frac{\text{Re}}{\kappa \text{Ma}} p - \mathbf{n} \cdot \boldsymbol{\tau} \cdot \mathbf{n} = \frac{1}{\delta} \frac{\text{Re}}{\text{We}} \nabla \cdot \mathbf{n} \quad (119)$$

yields (117b).

Since we are working on short distances from the plate edge, we can look for a solution in the form $v_r = r^n U(\theta)$ and $v_\theta = r^n V(\theta)$, which leads to two coupled ODEs:

$$U_{\theta\theta} + [n^2 + \chi(n^2 - 1)]U + \chi(n - 1)V_\theta = 0, \quad (120a)$$

$$(1 + \chi)V_{\theta\theta} + n^2V + \chi(n + 1)U_\theta = 0. \quad (120b)$$

Putting $(U, V) = (\widehat{U}, \widehat{V}) e^{m\theta}$, we get the quadratic determinant for finding m^2 :

$$(1 + \chi)m^4 + [2n^2(1 + \chi) - \chi]m^2 + n^2[n^2(1 + \chi) - \chi] = 0, \quad (121)$$

the solution of which is

$$m^2 = \left\{ -n^2, -n^2 + \frac{\chi}{1 + \chi} \right\}, \quad \text{i.e.,} \quad m_{1,2} = \pm i n, m_{3,4} = \pm i \sqrt{n^2 - \frac{\chi}{1 + \chi}}, \quad (122)$$

where it is clear that we are interested in $n > 0$ so that \mathbf{v} is nonsingular. The boundary conditions on U and V are

$$\text{(tangential)} \quad \theta = 0: U_\theta + (n - 1)V = 0, \quad (123a)$$

$$\text{(no-slip)} \quad \theta = -\pi: U = V = 0. \quad (123b)$$

From (120) we also find the relation between the amplitudes \widehat{U} , \widehat{V} :

$$\widehat{V} = -\frac{\chi m(n + 1)}{m^2(1 + \chi) + n^2} \widehat{U}, \quad (124)$$

or, more specifically, for each choice of m :

$$m_{1,2}^2 = -n^2: \quad \widehat{V}_{1,2} = -\frac{n + 1}{m_{1,2}} \widehat{U}_{1,2}, \quad (125a)$$

$$m_{3,4}^2 = -n^2 + \frac{\chi}{1 + \chi}: \quad \widehat{V}_{3,4} = \frac{m_{3,4}}{n + 1} \widehat{U}_{3,4}. \quad (125b)$$

Hence, the solution to (120) reads

$$\begin{pmatrix} U \\ V \end{pmatrix} = \sum_{i=1,2} \widehat{U}_i \begin{pmatrix} 1 \\ -\frac{n+1}{m_i} \end{pmatrix} e^{m_i \theta} + \sum_{i=3,4} \widehat{U}_i \begin{pmatrix} 1 \\ \frac{m_i}{n+1} \end{pmatrix} e^{m_i \theta}. \quad (126)$$

With the assumed form of the velocity field, the normal dynamic condition (117b) can be rewritten as

$$2h_r + r h_{rr} = \beta r^{n-1}, \quad (127)$$

with $\beta = \text{const} \sim \delta \text{We}/\text{Re}$. Hence,

$$h = \gamma r^n \quad \text{with} \quad \gamma = \frac{\beta}{2n + n(n - 1)}, \quad (128)$$

from where, again, it is clear that one needs $n > 0$ as h must tend to zero for $r \rightarrow 0$. If the interfacial deflection can be neglected at early times close to the plate edge (cf. Sec. IV D) for r 's in the range where the power law $v_r, v_\theta \sim r^n$, and $h \sim r^n$ is valid, then we get a fourth condition on U, V from (117b):

$$\text{(normal)} \quad \theta = 0: \gamma U + (\chi + 1)V_\theta = 0, \quad \text{with} \quad \gamma = 2 + (\chi - 1)(n + 1). \quad (129)$$

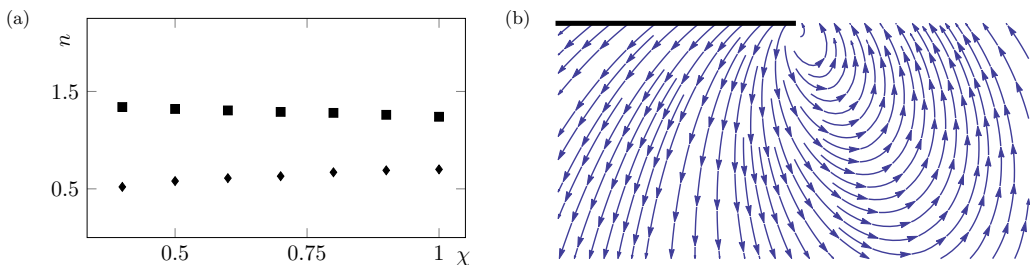


FIG. 8. Solution to the viscous compressible problem near the plate edge for early times: (a) branches of solutions $n(\chi)$ and (b) streamlines in the viscous compressible case for $\chi = 0.5$, $n \simeq 1.32427$.

Applying the boundary conditions (123a), (123b), and (129) to the solution (126) produces a homogeneous 4-dimensional system, the determinant of which must be equal to zero for a nontrivial solution to exist:

$$\begin{vmatrix} e^{-m_1\pi} & e^{-m_2\pi} & e^{-m_3\pi} & e^{-m_4\pi} \\ -\frac{n+1}{m_1}e^{-m_1\pi} & -\frac{n+1}{m_2}e^{-m_2\pi} & \frac{m_3}{n-1}e^{-m_3\pi} & \frac{m_4}{n-1}e^{-m_4\pi} \\ m_1 - \frac{n^2-1}{m_1} & m_2 - \frac{n^2-1}{m_2} & 2m_3 & 2m_4 \\ \gamma - (n+1)(\chi+1) & \gamma - (n+1)(\chi+1) & \gamma + \frac{m_3^2}{n-1}(\chi+1) & \gamma + \frac{m_4^2}{n-1}(\chi+1) \end{vmatrix} = 0. \quad (130)$$

Branches of solutions $n(\chi)$ are shown in Fig. 8(a) with a sample solution for $\chi = 0.5$ plotted in Fig. 8(b), demonstrating noticeable differences from the incompressible flow patterns in Fig. 4.

VI. CONCLUSIONS

In conclusion, let us review the regions of validity of the key inviscid incompressible (3) and compressible (83) approximations provided gravity (33), viscosity (38), and surface tension (51) effects are irrelevant. If we compare the conditions (45) and (92), it follows that in the region of interest, for a fixed ϵ with increasing time (horizontal arrow in Fig. 3), one first goes from the mostly undisturbed region as the shock wave has not yet propagated through the fluid, to the shock wave, the linear compressible, linear incompressible, then nonlinear incompressible, and finally compressible regimes again. At the latter stage, while the curve Ma^2/κ suggests that nonlinear effects should be important, the solution amplitude decays and hence this stage is no longer of interest in the context of resolution of singularities. Similar observations can be made for a fixed time κ with decreasing distance from the edge (vertical arrow in Fig. 3). The nonlinearity becomes important in the compressible case for $\epsilon \sim \text{Ma}^2/\kappa$ and in the incompressible case for $\epsilon \sim (\text{Ma}/\kappa)^{2/3}$; both limits are plotted in Fig. 3. The (lower) bounds on ϵ necessary for neglecting nonlinearity are different in the compressible and incompressible cases because the latter is more restrictive since it requires the incompressibility condition to be satisfied, which leads to (42), and hence its boundary is higher than that for compressible case. Viscous effects engage at the distance ϵ_{vis} given by (55a), which may happen in the compressible or incompressible regime depending on the relative values of κ , Ma , and Re . Finally, surface tension effects come into play when inequality (51) fails in both incompressible and compressible cases.

Because of the linear structure of the governing equations as justified by the physics of the impact phenomena at early times, the solutions at each of the key stages properly defined in the (t, r) plane by the relevant nondimensional parameters (Ma , Re , We , etc.)—viscous compressible (Sec. VC), viscous incompressible (Sec. IIIB), inviscid compressible (Sec. IVB), and inviscid incompressible (Sec. I)—can be constructed analytically with the help of a self-consistent asymptotic analysis. These solutions prove to be self-similar in the region near the plate edge, though with different forms of self-similarity and nonoverlapping regions of validity, thus making it impossible to recover one

solution from another (by taking limits), except for the incompressible case [19]. This means that in between these self-similar solutions in the (t, r) plane for a given set of nondimensional parameters there must exist non-self-similar solutions providing appropriate transition (matching), but they cannot be constructed analytically. The first three asymptotic solutions—viscous compressible, viscous incompressible, and inviscid compressible—resolve the corresponding singularities: the singularity at $t \rightarrow 0$ and $r \rightarrow 0$ is isolated in the sense that outside it one has the classical inviscid incompressible solution (3), but its singularity does not propagate to $t \rightarrow 0$ and $r \rightarrow 0$, where the physics unaccounted in the pressure-impulse theory resolves the singular behavior. In view of the characteristic properties of the problem, the dynamics is dominated by diffusion in the limit of short times, $t \rightarrow 0$, which leads to incompressible viscous equations, whose solution is responsible for the regularization of the singular limits $t \rightarrow 0$ and $r \rightarrow 0$ in the pressure-impulse theory. At the same time, depending on the nature of the impacted liquid, this “incompressible viscous” stage may require a deeper look at the submicroscopic physics when the NSEs are not applicable. Namely, the momentum (energy) diffusion and compressibility (sound, shock wave) propagation mechanisms can be different from those for liquids under normal conditions in view of the time scales below the relaxation period—the existence of transverse sound waves and phonon-type diffusion are among the processes atypical for normal conditions.

Questions requiring future study include energy and dimensionality effects. Namely, while in the present study we limited ourselves to the case of barotropic fluids, $p = p(\rho)$, it would be interesting to understand the thermodynamic aspects of the impact when the equation of state depends on temperature as well, $p = p(\rho, T)$, and thus the energy equation should be taken into account. Also, while we considered the 2D flow only, one may wonder how the crucial difference in the structure of the solution of the wave equation (106) between 2D and 3D—namely, the existence of sharp signals in 3D as opposed to the 2D case—affects the impact phenomena. One consequence of this is a stronger (lasting) effect of compressibility in 2D compared to that in 3D, which physically would be the flow around a corner of a 2D impactor plate [8]. The evolution of vorticity does not differ, however, between 2D and 3D since the linear vector equation (108) is the same regardless of the dimension.

While the phenomena studied here proved to be interesting due to the sudden change in the boundary conditions—from no penetration to the free boundary (2) in the inviscid case (exhibiting singularity) and from no-slip to the free boundary (62) in the viscous case (partially regularizing the singularity, i.e., the involved forces are still divergent)—substituting the no-slip by a slip condition in (62), as is common in the moving contact line problem, might represent a means of further regularization in the viscous case, in particular to make the forces finite. This could be especially relevant for the solid-liquid combinations yielding a substantial slip [51] such as in the case of polymer solutions or hydrophobic surfaces, i.e., whenever hydrodynamic shear can easily lead to molecular slip [52]. It must be noted, however, that in the moving contact line problem the no-slip condition leads to a singular shear stress even in the Stokes approximation versus our case as per Eq. (65). Dealing with the contact line singularity becomes a necessity in the case of impacts of blunt bodies and wedges, i.e., when there are moving contact lines. The latter type of impactors naturally should also exhibit the linear and nonlinear as well as the compressible and incompressible impact stages (albeit affected by the curvature or other geometric features of the impacting body) considered in the present paper, which deals with the most singular situation of impact phenomena—the flat plate impact problem.

ACKNOWLEDGMENTS

This work was partially supported by the National Science Foundation (NSF) CAREER Award No. 1054267 and the Natural Sciences and Engineering Research Council of Canada (NSERC) Grant No. 6186. The author also acknowledges stimulating conversations with A. Zelnikov and D. Labutin, helpful suggestions by anonymous referees, and careful reading of the manuscript by H. van Roessel.

APPENDIX A: ENERGY GAINED BY FLUID AFTER IMPACT

Note that regardless of whether the impacting plate is considered to have a finite or an infinite mass, the fluid gains only a finite energy; otherwise the whole idea of added mass [4] becomes invalid. Thus, the kinetic energy of all the fluid set in motion right after the impact is finite even though some parts of the impacted fluid (near the plate edges) move with an infinite speed, which is because the mass of those fluid parts is infinitesimally small and thus the contribution to the total kinetic energy of the entire semi-infinite fluid body is bounded. Therefore, the fact of an infinite mass and finite speed (and thus infinite kinetic energy) of the plate does not entail that the energy transferred to the fluid is infinite as well—in fact, it is finite and can be easily evaluated for the early stage of the impact, in which we are interested, by following the standard considerations [4] for the impact of a plate of width $2l$, cf. Fig. 1(a). Since the complex potential in the z plane is (3) and the impulsive pressure in a fluid right after the impact $P \equiv \int_{-0}^{+0} p dt = \rho\phi$, then on the plate $y = 0$ $P(z) = \rho \operatorname{Re} f(z) = \rho V_0 \sqrt{l^2 - x^2}$, so that we can find the impulsive force acting on the plate at the moment of impact:

$$F = \rho V_0 \int_{-l}^l \sqrt{l^2 - x^2} dx = \frac{\pi}{2} \rho V_0 l^2, \quad (\text{A1})$$

which should be equal to $F = m(V_{-0} - V_0)$ by Newton's second law, where V_{-0} is the plate velocity before the impact, in general different from the velocity $V_0 \equiv V_{+0}$ after the impact due to the plate finite mass m . Thus, because of the added fluid mass m_{add} equal to half-cylinder of the radius l (half-width of the plate), $(\pi l^2/2) \rho$ in (A1), the velocity of the plate decreases from V_{-0} to V_0 :

$$V_0 = \frac{m V_{-0}}{m + \frac{\pi \rho l^2}{2}}. \quad (\text{A2})$$

The momentum balance (A2) is applicable in the limit $m \rightarrow +\infty$ as well, which yields $V_{-0} = V_0$. To show that the energy acquired by the fluid is finite, append to the momentum balance (A2) the energy balance

$$\frac{m V_{-0}^2}{2} = \frac{m V_0^2}{2} + \frac{m_{\text{add}} V_{\text{ave}}^2}{2}, \quad (\text{A3})$$

which, when solved together with (A2), in the limit $m \rightarrow \infty$ gives for the average velocity $V_{\text{ave}} = \sqrt{2} V_{-0} = \sqrt{2} V_0$ of the added mass m_{add} , i.e., the energy acquired by fluid right after the impact is finite. Note that based on (3), the velocity decays as r^{-2} with distance from the origin and thus the energy decays as r^{-4} , which explains why the added mass is finite and the kinetic energy of the fluid acquired after the impact of a plate of an infinite mass is finite as well.

APPENDIX B: ON SELF-SIMILARITY OF THE WAVE EQUATION

The standard one-dimensional wave equation

$$\frac{\partial^2 \phi}{\partial t^2} = c^2 \frac{\partial^2 \phi}{\partial x^2} \quad (\text{B1})$$

has the obvious self-similar type symmetry, in which time and space coordinates are being stretched with equal rates, thus allowing one to look for a solution in the form

$$\phi = \phi(\eta), \quad \eta = \frac{t}{x}; \quad (\text{B2})$$

this means that the solution at the point (t, x) looks the same as at $(\alpha t, \alpha x)$, $\alpha > 0$. Substituting the above ansatz produces an ordinary differential equation

$$\frac{d^2\phi}{d\eta^2} = c^2 \left[2\eta \frac{d\phi}{d\eta} + \eta^2 \frac{d^2\phi}{d\eta^2} \right], \quad (\text{B3})$$

the solution of which is

$$\phi = C_1 + C_2 \ln \left(\frac{1 + c\eta}{1 - c\eta} \right). \quad (\text{B4})$$

Now, if one compares this self-similar solution to the general solution of (B1)

$$\phi = f(x - ct) + g(x + ct), \quad (\text{B5})$$

with some arbitrary functions f and g , it is clear that (B5) in general does not possess the same symmetry (B2) since $\phi = f(x - ct) + g(x + ct) = f[x(1 - c\eta)] + g[x(1 + c\eta)]$. Indeed, the ansatz $\phi = \tilde{f}(1 - c\eta) + \tilde{g}(1 + c\eta)$ satisfies (B1) only if $\tilde{g}(y) = -\tilde{f}(y) = \ln(y)$. This illustrates the basic fact that self-similar solution (B4) represents a subclass of a general solution set (B5).

APPENDIX C: COMPRESSIBLE INVISCID SOLUTION: SELF-SIMILAR STRUCTURE

When considering the water impact problem locally, near the plate edge, or, equivalently, assuming the plate to be semi-infinite, one expects the solution to be self-similar in view of the absence of an independent geometric length scale. The corresponding mixed boundary-value problem for the 2D wave equation

$$\frac{1}{c^2} \frac{\partial^2 \phi}{\partial t^2} = \frac{\partial^2 \phi}{\partial x^2} + \frac{\partial^2 \phi}{\partial y^2}, \quad (\text{C1a})$$

$$y = 0: \quad \frac{\partial \phi}{\partial y} = -V_0, \quad x < 0, \quad (\text{C1b})$$

$$\phi = 0, \quad x > 0, \quad (\text{C1c})$$

has an obvious affine symmetry group thus allowing the self-similar solution of the form

$$\phi(t, x, y) = c^2 t \Phi(\xi, \eta), \quad \xi = \frac{x}{ct}, \quad \eta = \frac{y}{ct}, \quad (\text{C2})$$

which produces the equation

$$(1 - \xi^2) \frac{\partial^2 \Phi}{\partial \xi^2} - 2\xi \eta \frac{\partial^2 \Phi}{\partial \xi \partial \eta} + (1 - \eta^2) \frac{\partial^2 \Phi}{\partial \eta^2} = 0 \quad (\text{C3})$$

of elliptic type in the region $\xi^2 + \eta^2 < 1$. This illustrates an interesting property: while the original problem (C1a) is hyperbolic, its restriction (C3) to a self-similar plane is elliptic. Applying the Chaplygin transformation

$$\xi = r \cos \theta, \quad \eta = r \sin \theta, \quad r = \frac{2\varrho}{1 + \varrho^2} \quad (\text{C4})$$

to Eq. (C3), we get the Laplace equation in the region $\varrho < 1$:

$$\varrho \frac{\partial}{\partial \varrho} \left(\varrho \frac{\partial \Phi}{\partial \varrho} \right) + \frac{\partial^2 \Phi}{\partial \theta^2} = 0, \quad (\text{C5})$$

the solution of which near the origin behaves as $\Phi \sim \varrho^{1/2}$ in analogy with the potential in the incompressible case (7)—reverting back to the original variables, we get the leading-order asymptotics (85) for the compressible case.

APPENDIX D: ON SEPARABILITY OF THE WAVE EQUATION

In search for a separable solution to (B1), we assume $\phi(t, x) = A(t)B(x)$, which yields

$$\frac{A_{tt}}{A} = c^2 \frac{B_{xx}}{B} = -\lambda^2, \quad (\text{D1})$$

and hence harmonic solutions for both $A(t)$ and $B(x)$:

$$A = C_1 e^{i\lambda t} + C_2 e^{-i\lambda t}, \quad (\text{D2a})$$

$$B = C_1 e^{i\lambda x/c} + C_2 e^{-i\lambda x/c}, \quad (\text{D2b})$$

i.e., only smooth (Taylor expandable) solutions and therefore only integer powers of t and x .

As an alternative, let us look for a solution of (B1) in a recursive manner, i.e.,

$$\phi(t, x) = \sum_i a_i x^{n_i} t^{m_i}, \quad (\text{D3})$$

where powers n_i and m_i are not necessarily integers. Substitution into (B1) gives the following conditions for two terms to balance:

$$n_i - 2 = n_j, \quad m_i = m_j - 2, \quad a_j m_j (m_j - 1) = c^2 a_i n_i (n_i - 1). \quad (\text{D4})$$

If we are looking for solutions such that $t \gg x/c$, then if, say, $n_j = 1/2$ and $m_j = 1/2$, such a term in the solution representation will be balanced by $n_i = 5/2$ and $m_i = -3/2$. This construction enables the existence of a solution $\phi(t, x) \sim t^{1/2} x^{1/2}$ with $t \gg x/c$, i.e., of the form (85).

APPENDIX E: POST SHOCK WAVE ASYMPTOTICS WITHOUT SURFACE TENSION

In nondimensional variables (16), the problem is formulated as follows:

$$y < 0: \quad (\text{bulk}): \quad \frac{\partial^2 \phi}{\partial t^2} = \Delta \phi = \frac{1}{r} \frac{\partial}{\partial r} \left(r \frac{\partial \phi}{\partial r} \right) + \frac{1}{r^2} \frac{\partial^2 \phi}{\partial \theta^2}, \quad (\text{E1a})$$

$$t = 0: \quad \phi = \phi_t = 0. \quad (\text{E1b})$$

$$y = 0: \quad (\text{plate}): \quad \frac{\partial \phi}{\partial y} \equiv -\frac{1}{r} \frac{\partial \phi}{\partial \theta} = -1, \quad |x| < 1, \quad (\text{E1c})$$

$$(\text{free surface}): \quad \phi(t, x) = 0, \quad |x| > 1. \quad (\text{E1d})$$

It is clear that due to the boundary condition at $y = 0$, $|x| < 1$, the solution is not separable. Hence, we will consider the ‘‘eigensolution’’ case for a half-infinite plate, i.e., focus only on the region near the plate edge, when the boundary condition (E1c) is replaced by $\phi_\theta = 0$ at $y = 0$, $x < 0$. Letting $\phi(t, r, \theta) = A(t)\Phi(r, \theta)$ with $\Phi(r, \theta) = B(r)C(\theta)$, we arrive at the following problems: for $A(t)$,

$$A_{tt} - \lambda^2 A = 0; \quad t = 0: \quad A = A_t = 0; \quad (\text{E2})$$

for $C(\theta)$,

$$C_{\theta\theta} + n^2 C = 0; \quad \theta = 0: \quad C = 0, \quad \theta = -\pi: \quad C_\theta = 0; \quad (\text{E3})$$

and for $B(r)$,

$$\frac{1}{r} \frac{d}{dr} \left(r \frac{dB}{dr} \right) - \left(\frac{n^2}{r^2} + \lambda^2 \right) B = 0, \quad (\text{E4})$$

which gives the solution in terms of modified Bessel functions

$$B(r) = C_1 I_n(\lambda r) + C_2 K_n(\lambda r), \quad (\text{E5})$$

where $K_n(\lambda r)$ is singular at the origin and should be discarded. Clearly, with the initial conditions taken into account, the solution is not separable, but if we are looking for a long time limit $t \gg r$, then the solution becomes separable. For that reason, it is convenient to solve the problem using the Laplace transform,

$$\mathcal{L}(\phi) \equiv \widehat{\phi}(\lambda) = \int_0^{+\infty} \phi(t) e^{-\lambda t} dt, \quad (\text{E6})$$

with the standard properties of the derivatives transformation:

$$\int_0^{+\infty} \frac{d\phi}{dt} e^{-\lambda t} dt = \lambda \widehat{\phi}(\lambda) - \phi(0), \quad \int_0^{+\infty} \frac{d^2\phi}{dt^2} e^{-\lambda t} dt = \lambda^2 \widehat{\phi}(\lambda) - \frac{d\phi}{dt}(0) - \lambda\phi(0). \quad (\text{E7})$$

The solution for $C(\theta)$ is clearly quantized because of (E3), thus giving

$$C(\theta) = \text{const} \cdot \sin\left(\frac{1}{2} + m\right)\theta, \quad m \in \mathbb{Z}. \quad (\text{E8})$$

If we are looking for the solution near the plate edge, $r \rightarrow 0$, then the asymptotics of $B(r)$ follows from that of $I_n(z) \sim (\frac{1}{2}z)^n / \Gamma(n+1)$.

Since we are interested in the asymptotics behind the shock wave, i.e., $t \gg r$, which in the Laplace space variable means $\lambda^{-1} \gg r$ or $\lambda r \ll 1$, and the asymptotics of the inviscid compressible flow should be consistent with the asymptotics of the inviscid incompressible flow for $r \ll 1$, i.e., $\phi \sim r^{1/2}$, then the leading-order term in the solution must correspond to $m = 0$:

$$\widehat{\phi} \sim \lambda^{1/2} r^{1/2} \sin \frac{\theta}{2}. \quad (\text{E9})$$

In order to recover the form of the solution in the physical space, note that the inverse Laplace transform \mathcal{L}^{-1} of $\lambda^{-1/2}$ is

$$\mathcal{L}^{-1}\left(\frac{1}{\sqrt{\lambda}}\right) = \frac{1}{\sqrt{\pi t}}, \quad (\text{E10})$$

so that by differentiating the solution (E9) in the Laplace space

$$\frac{d\widehat{\phi}}{d\lambda} \sim \lambda^{-1/2} \sim \int_0^{+\infty} t \phi(t) e^{-\lambda t} dt \quad (\text{E11})$$

and comparing with (E10), we recover (85).

APPENDIX F: ON THE PHYSICS OF DIFFUSION IN LIQUIDS

While it is understood how an infinite speed of propagation occurs in the macroscopic diffusion equation in the context of molecular diffusion (random walks) [53], the estimates of t_* and l_* in Sec. VB imply that under certain conditions, e.g., when $l_* = 10^{-9}$ m, diffusion processes need to be revisited in order to make a precise sense of the early times of the impact phenomena. First of all, it is known that the standard diffusion equation fails at such scales [54,55]. Second, diffusion of viscous effects is different from molecular diffusion since the former is momentum and energy transfer (as opposed to mass transfer), which puts it in the realm of heat transfer and thus the dominating physical mechanisms (phonons, electrons, photons, etc.) responsible for the diffusion differ from material (random walk) transport of molecular diffusion and depend on the nature of the liquid. In fact, the electromagnetic nature of the diffusion mechanisms allows faster than sound propagation speeds, at least on small scales.

Depending on the nature of a particular liquid system, there could be several mechanisms responsible for heat diffusion [49,56–58]—such as by phonons, molecular random walks, electrons, photons, etc.—each of which would have a different speed of propagation. Each process of heat diffusion is linear and therefore, if the heat was released at a point, leads to a Gaussian distribution. Since a linear combination of Gaussians is not a Gaussian, the system is in a nonequilibrium state due

to different carriers (phonons, molecules, electrons, photons, etc.) having different “temperatures”. Given the linearity of the phenomena, such a nonequilibrium heat diffusion described by several diffusion processes with different constant diffusion coefficients is qualitatively analogous to the process described by a single linear equation model with a time-dependent diffusion coefficient. For example, if we consider diffusion from the point source $\delta(x)$ on the real line $x \in \mathbb{R}$,

$$\frac{\partial u}{\partial t} = \epsilon t^\alpha \frac{\partial^2 u}{\partial x^2}, \quad (\text{F1a})$$

$$t = 0: \quad u(0, x) = \delta(x), \quad (\text{F1b})$$

where $\alpha > 0$, we find

$$u(t, x) = \frac{1}{2\sqrt{\pi c^2}} e^{-\frac{x^2}{4c^2}}, \quad \text{where } c^2 = \frac{\epsilon t^{\alpha+1}}{\alpha + 1}; \quad (\text{F2})$$

i.e., the diffusion propagates with speed $\sim \sqrt{\epsilon t^{\alpha+1}}$ as opposed to $\sim \sqrt{\epsilon t}$ in the constant diffusion-coefficient case, which means that the speed of propagation may vary from infinite to finite. While a macroscopic diffusion (viscosity) coefficient stands for the “front” (of the propagating quantity—energy, vorticity, etc.—defined in some averaged statistical sense), some of the underlying mechanisms propagate faster, though carrying only a portion of the energy. However, physically, this fact is important as the media is disturbed through viscous diffusion faster than the compression wave propagates into it. Later on, more energy is transferred, which effectively means that the viscosity coefficient is growing and thus time dependent. Another important note to make is that the mechanisms responsible for diffusion and sound propagation may overlap at submacroscopic distances—for example, there exists a ballistic mechanism [54,55,59] responsible for transport phenomena at scales comparable to the mean free path, which makes transport faster than the speed of sound [60], not to mention that at the time scales below relaxation phonons make it possible for the existence of both phonon-mediated diffusion and transverse sound waves otherwise absent in liquids on longer time scales [61].

-
- [1] T. H. von Karman, The impact on seaplane floats during landing, Tech. Rep. 321, NACA, 1929.
- [2] H. Lamb, *Hydrodynamics* (Cambridge University Press, New York, 1975).
- [3] L. G. Loitsyanskii, *Mechanics of Liquids and Gases* (Pergamon Press, New York, 1966).
- [4] M. A. Lavrentiev and B. V. Schabat, *Methoden der komplexen Funktionentheorie* (Deutscher Verlag der Wissenschaften, Berlin, 1967).
- [5] G. K. Batchelor, *An Introduction to Fluid Dynamics* (Cambridge University Press, New York, 1967).
- [6] M. A. Lavrentiev and M. V. Keldysh, General problem of impact on water, *Trudy TsAGI* **152**, 5 (1935).
- [7] The eigenvalue character of the solution stays valid in the viscous (and compressible) case as well since the no-slip condition at the plate wall along with the dynamic and kinematic conditions at the free boundary are homogenous. In particular, in the viscous setting, on the plate surface one amends (6a) to zero no-slip boundary condition $\theta = -\pi : v_r = v_\theta = 0$. Because of the homogeneous character of the involved boundary conditions, the solution accounting for compressible and viscous effects also has the meaning of an eigensolution.
- [8] R. Krechetnikov, Flow around a corner in the water impact problem, *Phys. Fluids* **26**, 072107 (2014).
- [9] One might argue that the velocity is infinite only for $t = +0$ and becomes finite for $t > 0$, so that the distance traveled by the interfacial point next to the plate must be finite or zero. However, inviscid flow around a plate edge stays singular for $t > 0$ same as a steady flow around a sharp corner [10].
- [10] L. D. Landau and E. M. Lifshitz, *Fluid Mechanics* (Pergamon Press, New York, 1987).
- [11] However, the bulk viscosity may become negative for media in thermodynamic nonequilibrium [62].
- [12] In the present study, we limit ourselves to the tangential departure of the free surface, though in general the contact angle the free surface makes with the plate is dictated by wetting properties, in particular.

- [13] P. G. Tait, Report on some physical properties of fresh water and seawater, in *The Voyage of H.M.S. Challenger* (Her Majesty's Government, London, 1888), Vol. 2, pp. 1–76.
- [14] The characteristic pressure is determined from the fact that the mass $\rho_0 l c_0 dt$ accelerates in time dt and thus the force acting during time dt (momentum change) is $\rho_0 l c_0 V_0 dt$.
- [15] Note that conceptually the weakly compressible limit is different from the *acoustic approximation* [63], which assumes that $Ma \ll 1$ and then neglects the initial stage when compressibility is important—in our case, however, we are focusing exactly on the initial stage when compressibility is important, but the density variation is still small, $|\rho| \ll \rho_0$. Hence, following the standard convention in the shock wave theory [10], instead of “acoustic wave” we will use the terms “compression wave” and “shock wave,” which necessarily must be weak.
- [16] Shock waves are known to form in nonlinear ideal fluid (not only gas) dynamics due to wave steepening or, equivalently, intersection of characteristics. However, discontinuities may also form even in the solutions of linear equations, when there are discontinuities in the initial and/or boundary conditions, as happens here.
- [17] G. V. Logvinovich, *Hydrodynamics of Free-Boundary Flows* (NASA/NSF, Washington, DC, 1972).
- [18] A. Iafrati and A. A. Korobkin, Initial stage of flat plate impact onto liquid free surface, *Phys. Fluids* **16**, 2214 (2004).
- [19] R. Krechetnikov, Origin of ejecta in the water impact problem, *Phys. Fluids* **26**, 052105 (2014).
- [20] In general, however, regularization of the solution of the NSEs by viscosity depends on the boundary conditions and the domain geometry and is not a guarantee such as in the moving contact line problem. It is not unusual for the leading-order asymptotics to be singular in problems with corners and/or mixed boundary conditions even in the full compressible NSEs treatment [64,65].
- [21] The limit $\varepsilon \rightarrow 0$ is singular in the sense of characteristics and speed of propagation as the order of equations changes when $\varepsilon = 0$ and characteristics of the inviscid problem become subcharacteristics of the viscous problem [66].
- [22] Y. L. Yakimov, Influence of atmosphere at falling of bodies on water, *Izv. Akad. Nauk SSSR, Mekh. Zhidk. Gaza* **5**, 3 (1973).
- [23] V. S. Vladimirov, *Equations of Mathematical Physics* (Mir, Moscow, 1984).
- [24] O. A. Ladyzhenskaya, *Mathematical Theory of Viscous Incompressible Flow* (Gordon and Breach, New York, 1969).
- [25] I. R. Peters, D. van der Meer, and J. M. Gordillo, Splash wave and crown breakup after disk impact on a liquid surface, *J. Fluid Mech.* **724**, 553 (2013).
- [26] L. A. Galin, Impact of solid body on a compressible liquid surface, *Prikl. Mat. Mekh.* **11**, 547 (1947).
- [27] F. Frank and R. von Mises, *Differential and Integral Equations of Mathematical Physics* (United Scientific and Technical Press, Moscow-Leningrad, 1937).
- [28] L. A. Galin, A wing rectangular in plan in a supersonic flow, *Prikl. Mat. Mekh.* **11**, 465 (1947).
- [29] L. M. Flitman, On a mixed boundary value problem for the wave equation, *J. Appl. Math. Mech.* **22**, 1185 (1958).
- [30] S. G. Mikhlin, Several elementary boundary value problems for the wave equation, *Trudy Seismologicheskogo instituta, Akad. Nauk SSSR* **101**, 1 (1940).
- [31] T. F. Ogilvie, Compressibility effects in ship slamming, *Shiffstechnik* **10**, 147 (1963).
- [32] V. Kubenko, *Penetration of Elastic Shells in a Compressible Liquid* (Naukova Dumka, Kiev, 1981).
- [33] A. Sagomonian, *Penetration of Solid Bodies in a Compressible Liquid* (Moscow University Press, Moscow, 1974).
- [34] S. R. Brinkley and J. G. Kirkwood, Theory of the propagation of shock waves, *Phys. Rev.* **71**, 606 (1947).
- [35] G. Taylor, The formation of a blast wave by a very intense explosion. I. Theoretical discussion, *Proc. Roy. Soc. London, Ser. A* **201**, 159 (1950).
- [36] S.-C. Lin, Cylindrical shock waves produced by instantaneous energy release, *J. Appl. Phys.* **25**, 54 (1954).
- [37] M. F. M. Osborne and A. H. Taylor, Non-linear propagation of underwater shock waves, *Phys. Rev.* **70**, 322 (1946).
- [38] R. H. Cole, *Underwater Explosion* (Princeton University Press, Princeton, NJ, 1948).

- [39] G. I. Barenblatt, *Scaling, Self-Similarity, and Intermediate Asymptotics* (Cambridge University Press, New York, 1996).
- [40] C. Truesdell, *The Kinematics of Vorticity* (Indiana University Press, Bloomington, IN, 1953).
- [41] G. B. Arfken and H. J. Weber, *Mathematical Methods for Physicists* (Academic Press, San Diego, CA, 2005).
- [42] I. G. Petrovsky, *Partial Differential Equations* (Interscience Publishers, New York, 1954).
- [43] R. von Mises, On the thickness of a steady shock wave, *J. Aeronaut. Sci.* **17**, 551, 594 (1950).
- [44] D. Gilbarg and D. T. Paolucci, The structure of shock waves in the continuum theory of fluid, *J. Rat. Mech. Anal.* **2**, 617 (1953).
- [45] H. Weyl, Shock waves in arbitrary fluids, *Commun. Pure Appl. Math.* **2**, 103 (1949).
- [46] W. M. Haynes, *CRC Handbook of Chemistry and Physics* (CRC Press, Boca Raton, FL, 2014).
- [47] J. Frenkel, *Kinetic Theory of Liquids* (Oxford University Press, Oxford, UK, 1947).
- [48] L. D. Landau and E. M. Lifshitz, *Statistical Physics* (Nauka, Moscow, 1964).
- [49] F. S. Gaeta, Radiation pressure theory of thermal diffusion in liquids, *Phys. Rev.* **182**, 289 (1969).
- [50] Following these original ideas of Frenkel [47], Bolmatov *et al.* [56] recently developed a phonon like theory to calculate the thermodynamic properties of liquids (the phonon like modes are understood in the sense that they are not entirely harmonic vibrations as in crystals, but instead eigenstates in topologically disordered liquids—the heat content in liquids is a sum of both kinetic and potential energies similar to solids—as shown by Trachenko and Brazhkin [61], the contribution of vibrational modes dominate over that of diffusion which justifies the use of the phonon-based theory for liquids).
- [51] E. Lauga, M. Brenner, and H. Stone, Microfluidics: the no-slip boundary condition, in *Springer Handbook of Experimental Fluid Mechanics*, edited by C. Tropea, A. L. Yarin, and J. F. Foss (Springer-Verlag, Berlin, 2007), pp. 1219–1240.
- [52] Under normal conditions, water (molecular diameter 0.29 nm, the mean free path 0.25 nm, and the intermolecular spacing 0.4 nm) does not exhibit a significant slip, only on the order of the mean free path, which makes it similar to the length l_* estimated in Sec. VB. Glycerin also does not exhibit a significant slip (molecular radius 0.435 nm, the intermolecular spacing 0.428 nm), in which case the length l_* estimated in Sec. VB is much larger than the mean free path. Given these observations, in the process of revising the paper, a resolution to the moving contact line singularity was offered [67]. Namely, significant viscous stresses at the contact line lead to thermal dissipation, which in turn establishes a surface tension gradient along the liquid-air interface, leading to bulging of the latter away from the ideal wedge geometry considered by Moffatt [68] and Huh and Scriven [69]. The interface deformation continues until balanced by the capillary pressure, thus creating a region of high curvature, so that the interface meets the substrate at the submicroscopic contact angle π , thereby removing the contact line singularity.
- [53] J. B. Keller, Diffusion at finite speed and random walks, *Proc. Nat. Acad. Sci. USA* **101**, 1120 (2004).
- [54] A. A. Joshi and A. Majumdar, Transient ballistic and diffusive phonon heat transport in thin films, *J. Appl. Phys.* **74**, 31 (1993).
- [55] G. Chen, Ballistic-diffusive equations for transient heat conduction from nano to macroscales, *Trans. ASME* **124**, 320 (2002).
- [56] D. Bolmatov, V. V. Brazhkin, and K. Trachenko, The phonon theory of liquid thermodynamics, *Sci. Rep.* **2**, 421 (2012).
- [57] A. E. Steam, E. M. Irish, and H. Eyring, A theory of diffusion in liquids, *J. Phys. Chem.* **44**, 981 (1940).
- [58] E. L. Dougherty Jr. and H. G. Drickamer, A theory of thermal diffusion in liquids, *J. Phys. Chem.* **23**, 295 (1955).
- [59] G. Chen, Ballistic-diffusive heat-conduction equations, *Phys. Rev. Lett.* **86**, 2297 (2001).
- [60] The fact that the speed of molecules is faster than that of sound is easy to see with the example of monoatomic gases, i.e., $c_{\text{molecule}} = \sqrt{3kT/m}$ vs $c_{\text{sound}} = \sqrt{\gamma kT/m}$, where $\gamma = C_p/C_v < 3$.
- [61] K. Trachenko and V. V. Brazhkin, Duality of liquids, *Sci. Rep.* **3**, 2188 (2013).
- [62] N. E. Molevich and A. N. Oraevskii, Sound viscosity in media in thermodynamic disequilibrium, *Sov. Phys. JETP* **67**, 504 (1988).
- [63] A. A. Korobkin, *Impact of Liquid and Solid Masses* (Russian Acad. Sci., Novosibirsk, 1997).

- [64] J. R. Kweon and R. B. Kellogg, Regularity of solutions to the Navier-Stokes system for compressible flows on a polygon, [SLAM J. Math. Anal.](#) **35**, 1451 (2004).
- [65] J. R. Kweon and R. B. Kellogg, Regularity of solutions to the Navier-Stokes equations for compressible barotropic flows on a polygon, [Arch. Rat. Mech. Anal.](#) **163**, 35 (2002).
- [66] J. D. Cole, *Perturbation Methods in Applied Mathematics* (Blaisdell, Waltham, MA, 1968).
- [67] R. Krechetnikov, On the moving contact line singularity, [arXiv:1804.05169](#).
- [68] H. K. Moffatt, Viscous and resistive eddies near a sharp corner, [J. Fluid Mech.](#) **18**, 1 (1964).
- [69] C. Huh and L. E. Scriven, Hydrodynamic model of steady movement of a solid/liquid/fluid contact line, [J. Colloid Interface Sci.](#) **35**, 85 (1971).